Eastern Region Technical Attachment
No.2023-01
November 2023

Flash Flood Statistical Models for Predicting the Stage Heights on the Rocky Branch Creek in Downtown Columbia, SC

Anthony Petrolito, Leonard Vaughan, and Nicole Rebarick
NOAA/National Weather Service
Columbia South Carolina

Abstract

The Rocky Branch Creek watershed in downtown Columbia, South Carolina is prone to flash flooding on short time scales in convective heavy rain events. Rainfall runoff is enhanced due to both a significant elevation gradient in the basin and impervious urban land cover. The creek flows through a highly urbanized and commercial district known as Five Points and the southern portion of the University of South Carolina campus before it enters the Congaree River. Using upstream observed rainfall and response time as predictors, multiple linear regression models were developed to predict the stage heights at two locations on the creek: Main Street at Whaley Street and Pickens Street. The purpose of the models is to aid National Weather Service forecasters in flash flood warning decision-making by providing timely stage height predictions in near real time. A computer application was developed to ingest the predictor data in a timely manner and display forecast crest stages on the Rocky Branch Creek to the forecasters. It is hoped that this research will lead to an increase in flash flood warning lead times for the city of Columbia.

1. Introduction

Flash flooding along Rocky Branch can occur at any time of the year. However, there are certain months when the ingredients for flash flooding are more prevalent. Although this study only looked at six years of data from 2017 through 2022, the climatology of flood events was rather consistent. The months from May through August were the most active in the basin with the peak occurring during June and July. When looking at the 32 cases that reached flood stage, (7.2 feet) at Rocky Branch at Whaley and Main Streets, three months stood out. The months of May, June, and July accounted for 66% of all cases out of 8 months that reached flood stage in the 6-year developmental sample. During the summer season, hot, humid, and conditionally unstable conditions are often dominant. The combination of slow-moving thunderstorms, high precipitable water values (PW), and colliding outflow boundaries have the potential to produce locally heavy rainfall with intense precipitation rates. By only looking at the events that produced flash flooding, the months of January, February, October, and December had zero cases (Figure 1).

The Rocky Branch watershed in downtown Columbia, South Carolina is more complex than just terrain and urbanized areas. The watershed is small, encompassing just over four square miles. Within these four miles, there are several streamflow entry points and varying elevation, especially in the northern part of the watershed. This area is also defined by the highly-developed areas of the surrounding university and urban downtown, much of which contributes to the imperviousness of the basin. The steep terrain is especially noticeable upstream from the U.S. Geological Survey (USGS) stream gauge located at the intersection of Whaley and Main Streets. The creek falls approximately 100 feet from the upper portion of the basin near Millwood Avenue to where it empties into the Congaree River near the Vulcan Material quarry (Figures 2 and 3). In addition, plentiful impervious surfaces and a very extensive stormwater sewer system throughout the watershed will often increase stormflow volumes (Figure 4). The creek is most susceptible to significant flash flooding during convective rainfall events impacting areas from the Five Points District to the Olympia Neighborhood (Ress et al. 2020). Flash flood warnings (FFWs) from 2008-2022 and a heat map of flash flood Local Storm Reports (LSR's) from 2008-2022 within the WFO Columbia (CAE) county warning area (CWA) are shown in Figures 5a and 5b. The majority of both FFWs and flash floods (LSRs) occur over the Congaree River Basin. During heavy rainfall events, the stream responds very quickly as seen in Figures 6 and 7. As a result, in these situations, National Weather Service (NWS) forecasters often need to make quick decisions for the possible issuance of a Flash Flood Warning (FFW) with only a limited amount of time before flooding can occur. The developmental data set reinforced by forecaster experience shows that flash flooding can occur at Whaley and Main Streets in as little as 30 to 60 minutes from the onset of heavy rain.

Until the 1890s, the area in the upper watershed now known as the Five Points District was made up of farmland, woods, and swampland. By 1915, as the city of

Columbia continued to expand, a decision was made to further develop this area by burying the stream underground through large culverts (Helsley 2015). Rocky Branch flows through these culverts from Martin Luther King Park (MLK), once known as Valley Park, to Maxcy Gregg Park (ROCA). The infrastructure has been improved several times, but still contributes to the complex flows. Rocky Branch is now highly urbanized with surprisingly steep slopes, with elevations that range from 80 feet to 100 feet above the stream bed. This is most likely due to its location along the Fall Line and Sandhills region of South Carolina.

Numerous data sets are available to improve flash flood forecasting including both within the Advanced Weather Interactive Processing System (AWIPS) and online. Some of the useful tools include: The quantitative precipitation estimates from the Multi-Radar/Multi Sensor System (MRMS; Zhang et al. 2016) including Flooded Locations and Simulated Hydrographs (FLASH; Gourley et al.; 2017), and the Flash Flood Monitor and Prediction (FFMP; Filiaggi et al. 2002 and Smith et al. 2008). The HydroViewer Advanced application Gant (2020) available to NWS forecasters is quite useful because it incorporates several of these data sets into one display which facilitates flood potential diagnosis and overall situational awareness. Various mesonet rainfall data are available to NWS forecasters in near real time: The NWS Inter-Regional Integrated Services (IRIS) database, private sector and government data sets including the USGS, Richland County South Carolina Mesonet (RCWINDS), and rainfall data through the City of Columbia South Carolina monitoring network system maintained by Woolpert. However, due to the rapid response of the creek to rainfall in the upstream headwaters of the watershed and the various data sets to examine, long FFW lead times have been difficult to achieve. Therefore, to improve the FFW decision making and verification, statistical models were developed to predict the stage height on the creek using upstream rain gauges that are available to NWS forecasters in real time. Two linear regression models were developed, Rocky Branch at Whaley Street (RBWS1) and Rocky Branch at Pickens Street (RBPS1). The goal of this research was to provide timely stage height predictions to the forecasters to aid the warning decision making process, ultimately increasing the lead time of the FFWs for this vulnerable area. Additionally, better guidance should help maintain low false alarm rates.

2. Data and Methodology

The developmental data set for the RBWS1 model consisted of 86 cases from the spring of 2017 through the summer of 2022. The data for the study are shown in Appendix 1. The developmental data set for the RBPS1 model was smaller and consisted of 58 cases from the fall of 2018 through the summer of 2022. A stepwise multiple linear regression was used to predict the stage height on the Rocky Branch creek at both Main Street at Whaley Street and at Pickens Street in Columbia, South Carolina. The least-squares methodology, the process of minimization of the sum of the squared errors (residuals), was used to fit the regression line. The residuals were assumed to be independent of each other with zero mean, constant variance and

normally distributed. A comprehensive explanation of least-squares regression can be found in Draper and Smith (1998), Neter et al. (1996) and Chatterjee et al. (2000). A less mathematically rigorous explanation of least-squares regression but with a focus on meteorological applications can be found in Wilks (1995). This study used the R software environment for statistical computing and graphics to perform the variable selection and multiple linear regression to predict the stage heights (R Core Team 2020). Some of the figures were produced using the R package ggplot2 (Wickham 2009). The potential predictor variables for both equations included upstream Woolpert rain gauges at MLK and ROCA (see Fig. 3), the cumulative rain duration time to crest in minutes (DMLK, DROCA), the precipitable water (PW) from the Rapid Refresh model (RAP) (Benjamin et al. 2016), and the seasonal time of year (Y). To determine the cumulative rain duration time, the data from the two rainfall locations (MLK and ROCA) were generated at 5 minute increments. The study did not restrain each event by the duration of the event. As seen in Appendix 1, the duration of each event was exclusive. For each case, the beginning and ending time of each event was based on when the heavy rain began and ended. Looking at each individual event, if the events that began and ended with multiple 5 minute reports of very light precipitation (i.e., 0.01 inches), these data and time periods were excluded from the totality of the event. The duration and intensity of the rainfall were the main components contributing to the urban flooding.

The objective of the variable selection procedure was to maximize the amount of variance explained by the predictor variables (coefficient of determination R^2) while at the same time minimize the amount of bias in the resultant stage height forecast (Mallows Cp). Scatter plots and histograms of the residuals were examined to determine if they exhibited normality and homoscedasticity (constant variance of the residuals). These are two important assumptions of multiple linear regression (Wilks 1995). In addition, the standardized residuals greater than the absolute value of 3 were examined as potential outliers (Chatterjee et al. 2000).

3. Results

For RBWS1, the original model selected after stepwise regression consisted of four predictors: ROCA, DROCA, MLK and PW (Figure 8). There was concern that the PW predictor coefficient was negative. This was surprising since meteorologically it was assumed that an increase in precipitable water should lead to heavier rain and an increased flash flooding potential in the basin. In addition, the PW was not a statistically significant predictor with a p-value greater than 0.05 and not correlated with the response variable. A scatter plot of PW vs. RBWS1 and the box and whisker plot of PW are shown in Figures 9a and 9b. PW greater or equal to 1.50 in. accounted for 88% of the cases and the 25th percentile was 1.68 in. However, since the PW was determined to be an extraneous predictor, it was removed and the model re-derived. The final RBWS1 model selected included the remaining three predictors: ROCA, DROCA, and MLK. ROCA and MLK were highly correlated with the response variable (Figures 10a and 10b).

*RBWS1 = 5.068282 + (1.879719 * ROCA) – (0.023158 * DROCA) (1.450731 * MLK)* **(1)**

The equation (1) statistical details, histogram, box and whisker plot of the residuals, and the Quantile-Quantile (QQ) plot are shown in Figures 11-13. The three independent predictor variables had very low p-values and therefore suggested high predictive value and statistical significance. The adjusted R^2 was 0.81. The histogram of the residuals and QQ plot suggested a symmetrical distribution with positive kurtosis and outliers.

One important assumption of multiple linear regression is that the predictor variables are independent from each other and therefore not redundant. If this is not the case, the regression coefficients can become poorly estimated leading to inflation of the variances and therefore unreliable (Draper and Smith 1998). Also, the associated p-values can become questionable undermining the perceived statistical significance of the predictors and the overall model (Neter et al. 1996 and Chatterjee et al. 2000). The variance inflation factor statistic (VIF) was examined to determine the level of mutual correlations (multicollinearity) between the predictor variables. The VIF calculation involves regressing each predictor variable on the other predictor variables and examining the resulting R^2. A higher value of R^2 corresponds to a higher value of the VIF (Chatterjee et al. 2000). ROCA had a VIF of 6.96 and MLK had a VIF of 6.86. A maximum VIF in excess of 10 is often used as a benchmark that collinearity is a significant problem in the response variable estimation although this value is somewhat arbitrary (Chatterjee et al. 2000, Draper and Smith 1998 and Neter et al. 1996). In most cases, a level of collinearity with a VIF below 10 does not affect inferences about mean predictions as long as the inferences are made within the overall scope of the model (Neter et al. 1996). A scatter plot of the ROCA and MLK observations showed that most fell within a jointly defined region which defined the overall scope of the model (Figure 14). Based on the scatter plot of the predictor variable observations between ROCA and MLK and the corresponding VIF for both predictors, it was determined that the degree of collinearity appeared not to be detrimental to the model to make reasonable inferences about the mean responses or predictions. An alternate equation was developed with MLK removed. However, this model exhibited a potential significant high bias with poor model fit as suggested by an inflated Cp statistic. The alternate model was under-fitted with the possibility of important predictors missing (Draper and Smith 1998). Since observational experience suggested the importance of the upstream rain gauge (MLK) in predicting the RBWS1 stage height, it was determined to use both ROCA and MLK as predictors in the model despite the relatively high collinearity between the two rain gauges and equation (1) was chosen to predict the stage height at RBWS1.

For RBPS1, the model selected after stepwise regression consisted of three predictors: DROCA, MLK, and DMLK. However, DROCA and DMLK predictors were not statistically significant, and the box plot of the residuals displayed negative skewness and outliers. The re-derived model consisted of two predictors: MLK and DMLK. MLK was highly correlated with the response variable (Figure 15).

*RBPS1 = 5.537181 + (2.410524 * MLK) – (0.019183 * DMLK)* **(2)**

The equation (2) statistical details, histogram, box and whisker plot of the residuals, and the Quantile-Quantile (QQ) plot are shown in Figures 16-18. The two independent predictor variables had very low p-values and therefore suggested high predictive value and statistical significance. The adjusted R^2 was 0.83. Of concern was that the distribution of residuals indicated non-normality of the response variable with the histogram showing negative skewness with positive kurtosis despite removing some outliers. Therefore, a square transformation of the response variable (y^2) was performed and an alternative model was developed (RBPS1A). The transformation improved the overall normality of the data as seen in the histogram of residuals although negative skewness remained likely influenced by extreme outliers. Since the developmental data set was small, it was decided not to remove any more outliers.

*RBPS1A = Sqrt (25.03815 + (38.03702 * MLK) – (0.24669 * DMLK))* **(3)**

The equation (3) statistical details, histogram, box and whisker plot of the residuals, and the Quantile-Quantile (QQ) plot are shown in Figures 19-21. The two independent predictor variables had very low p-values and therefore suggested high predictive value and statistical significance. The adjusted R^2 was 0.89. The distribution of residuals of the transformed equation still showed negative skewness with significant outliers, however the skewness had been reduced and the mean was closer to the median suggesting a more normal distribution and improvement from equation 2. Therefore, the transformed equation (3) was chosen as the model to predict the stage height at RBPS1. Although the R^2 for RBPS1 was higher than the value for RBWS1, the developmental data set for RBPS1 was smaller than RBWS1 and the normality of the residuals remained in question with significant outliers present. In addition, the RBPS1 equation was less robust than the RBWS1 equation despite the collinearity issue with RBWS1. Since the distribution of the residuals remained negatively skewed, the model was biased and not homoscedastic. And, given the extreme negative residual outliers, the model was expected to occasionally overestimate the stage crest heights.

The outliers for both models were further examined for leverage and influence using the Hat Matrix, DFFITS and Cook's Distance statistics. For the RBWS1 model, two outlier cases (12 and 83) had fairly strong leverage and moderately high influence. But the cases were not removed from the developmental data set since removing them resulted in little change in the predictor coefficients and statistical significance (Neter et al. 1996). The RBPS1 model had several outliers that had standardized residuals greater than 3 (in absolute value) given the non-normality of the developmental data. A few of them exhibited strong leverage and high influence with a noticeable change in the predictor coefficients after removing them. It is important to note that the models did not incorporate rainfall rates, and this may have contributed to the errors leading to outliers. The stage height forecast accuracy for longer duration rainfall events will be more impacted by not accounting for rainfall rates than the short duration events (less than 30

minutes) given the greater uncertainty. The models may also produce less reliable (over-forecast) stage crest forecasts especially for longer duration heavy rain events as suggested by the negative skewness of the RBPS1 model. This may be due to the fact that the Rocky Branch Creek is shallow and the predicted stage crests for those events are not realized before the water overflows the creek bed. In essence, the streamflow follows a logarithmic curve spreading across the basin. The investigation of outliers also suggested the importance of antecedent conditions on streamflow. There were outlier cases with observed stage crests above flood stage associated with low rainfall amounts at both ROCA and MLK. Further investigation of the cases revealed more significant rainfall accumulation occurred in the basin hours earlier and were not incorporated into the models.

A large enough independent data set to perform a quantitative analysis on the skill of the models to predict the stage heights at RBWS1 and RBPS1 was not available. However, two independent cases not included in the model development were examined to review model skill and potential FFW lead times: The 4 July 2022 and 18 July 2022 high water cases. The 4 July 2022 case resulted in the highest recorded crests at both RBWS1 (12.90 ft.) and RBPS1 (13.43 ft.). The 18 July 2022 case resulted in crests of 10.11 ft. at RBWS1 and 8.93 ft. at RBPS1. The cases were examined using the Storm Prediction Center (SPC) mesoanalysis archive (Bothwell et al. 2002), the High Resolution Ensemble Forecast (HREF) system graphics available from the SPC (Roberts et al. 2019), and the 5-minute archived Woolpert rainfall data at ROCA and MLK.

3.1 4 July 2022

On the morning of 4 July 2022, a weak and diffuse stationary front was located across central and northeast South Carolina which provided weak convergence across the area. Convection developed early in the day along the coast of South Carolina and flash flooding was observed in the Myrtle Beach area along a sea breeze boundary by around 1545 UTC (Figure 22). The convection was organized across eastern South Carolina along the sea breeze boundary between 1900 UTC and 2000 UTC. The 1200 UTC Radiosonde (RAOB) sounding for CHS indicated moderate instability in a weakly-sheared environment with surface-based Convective Available Potential Energy (CAPE) near 2000 J/kg. In addition, the precipitable water was around 2.00 inches, which was higher than the 75th percentile for the date. Thus, the collective CHS sounding data suggested an increased potential for heavy rain (Figure 23).

By 2100 UTC, with strong diabatic heating and increasing moisture, the air mass near Columbia, SC became very unstable with the surface-based CAPE increasing to near 3000 J/kg. As the sea breeze outflow boundary propagated westward as seen in the surface theta plot, the moisture convergence strengthened and precipitable water increased to around 2.25 inches (Figures 24 and 25). The 1200 UTC run of the convection-allowing models (CAMS) from the HREF suggested thunderstorms would develop along the coast then increase in

coverage and propagate into central South Carolina by 2200 UTC (Figures 26 and 27).

The MRMS radar reflectivity lowest scan product valid at 2130 UTC and 2200 UTC indicated thunderstorms developed near downtown Columbia north of the Whaley District before merging near the headwaters of the Rocky Branch basin (Figure 28). The convection eventually progressed southwest across the watershed. Both of the statistical models predicted a rapid rise in stage heights on Rocky Branch due to very efficient rain and training as seen in Table 1. With the MRMS radar data showing high reflectivity and training across the basin, the data suggested a FFW could have been issued as early as 2135 UTC since the volume of water was likely to only increase during the next several minutes. By 2140 UTC, the RBPS1 model predicted stage height was 7.03 ft, which would be near flood stage (7.2 ft.). Based on the statistical model output, forecaster confidence of flash flooding would be high. The stage heights were forecast to rise above flood stage at 2145 UTC, 7.65 ft. at RBWS1, and 8.27 ft. at RBPS1. The FFW was issued at 2150 UTC and the resulting warning polygon and radar composite reflectivity is shown in Figure 29. By using the statistical models, the lead time could have been extended 10 to 15 minutes. NWS forecasters can often further extend lead times by noting convective trends in the upstream basin. The RBWS1 gauge crested at 12.9 ft. while the model predicted a crest at 18.79 ft. Although the model over-forecasted the crest, the guidance provided timely information for the stage rising above flood stage. The RBPS1 gauge crested at 13.43 ft. while the model predicted a crest at 13.70 ft. So, the RBPS1 model crest height prediction was quite reasonable. The observed hydrographs for RBWS1 and RBPS1 are shown in Figure 30 along with model stage crest forecast heights and times.

It was interesting that the response time downstream at RBWS1 was faster than at RBPS1 (delayed 1-hr) given that the heaviest rain developed in the upstream basin associated with the storm cell merger, as detailed previously. Heavy rain to the north of the Whaley District in higher terrain prior to the storm cell merger may have been the impetus for the rapid rise at RBWS1 before RBPS1. It is important to note the stormwater sewer system in and around the Five Points District is more dense than downstream, especially just before the Whaley District. Additionally, the majority of the area encircling ROCA is a maintained park characterized by permeable soil, grass, and diverse vegetation, including some wetland foliage. This is a distinct contrast to the multiple urban university buildings, large asphalt parking lot, and single drainage basin surrounding Whaley. Combined with runoff from the headwaters downtown where the imperviousness is greater, the stormwater flow below ROCA likely increased significantly after the storm cell merger. These effects possibly accounted for the faster response time and higher crest at RBWS1 (Ress et al. 2020). One other hypothesis for the lag in the stream peaking upstream at Pickens Street versus downstream at Whaley Street could be the size of the culvert for Rocky Branch Creek to flow beneath Pickens Street. The culvert does not allow the stream at high levels to flow freely by constricting the flow beneath the roadway. The creek must overcome the culvert and embankment before it can

overflow the roadway and then back into the natural stream channel.

3.2 18 July 2022

On the morning of 18 July 2022, a surface ridge was off the South Carolina coast and an upper-level trough was located across the middle Mississippi River Valley. A surface cold front was located ahead of the upper trough from the Ohio Valley southwest to the Plains. The 1200 UTC RAOB from CHS indicated moderate instability with surface-based CAPE near 1000 J/kg (Figure 31). The precipitable water was a little higher than the 4 July case at 2.17 inches and a deep "warm" cloud depth (3.7 km) was present. Deep south-westerly flow aloft supported high precipitation efficiencies by limiting dry air entrainment and promoted heavy rain due to warm-rain collision-coalescence (Petersen et al. 1999). In addition, to put this case into a greater historical context, the precipitable water for this case was higher than the 90th percentile for the date.

With strong diabatic heating and deep moisture, the air mass became very unstable by 2000-2100 UTC across central South Carolina with surface-based CAPE values around 2500 J/kg and weak convergence being noted (Figure 32). The 0000/1200 UTC runs of the HREFS focused organized thunderstorm development across northwest Georgia into the Upstate of South Carolina late in the day ahead of a mid-level short wave trough with scattered disorganized thunderstorms across central South Carolina (Figures 33 and 34). However, a multicellular convective cluster developed in the South Carolina Piedmont near a theta-e boundary between 1700-1900 UTC (Figure 35). From there, thunderstorms moved northeast into the higher theta-e air across central South Carolina and organized into a line around 2000 UTC.

The MRMS radar reflectivity lowest scan product valid at 2050 UTC and 2110 UTC indicated the line of thunderstorms intensified near the downstream Rocky Branch basin and briefly trained to the headwaters before moving to the east by 2115 UTC (Figure 36). The heavy rain occurred over a 15-minute period with very efficient rainfall and runoff dominating the rapid response at RBWS1, shortly after 2055 UTC; while the response at RBPS1 was delayed until 2110 UTC. Based on the data from both models, the FFW decision could have been made as early as 2055 UTC as heavy rain developed in the downstream basin and the forecast stage at RBWS1 rose above flood (7.3 ft.) (Table 2). The model stages at both RBWS1 and RBPS1 were predicted to rise well above flood stage by 2100 UTC, but the FFW was issued at 2105 UTC (Figure 37). However, through integrating our newer model guidance into the decision-making process, the lead time could have been extended 10-15 minutes. The RBWS1 gauge crested at 10.11 ft. while the model predicted a crest at 9.96 ft. The RBPS1 gauge crested at 8.93 ft while the model predicted a crest at 8.64 ft. So both models predicted timely and reasonable stage heights at both locations for this case. The observed hydrographs for RBWS1 and RBPS1 are shown in Figure 38 with model forecast crest stage heights and times.

To simplify and facilitate the flash flood warning decision process, a Python application was developed in AWIPS to

display the forecast crest stages to NWS forecasters from the models resulting from this research. The predictor data for both models are ingested from the AWIPS Hydro Database at 5-minute intervals and the forecast crest stages are updated automatically. This allows forecasters to calculate the predicted stage height on-the-fly, seamlessly and quickly. The Python application our team developed utilizes the Python Tkinter toolkit for simplicity and efficiency as it populates the forecast stage even when idle. The forecaster also has the option of manually updating the rainfall and duration from Woolpert, giving users the ability to create a "what-if" scenario. Using the application should eliminate the cumbersome process of monitoring the rainfall data from Woolpert via their website and allow the NWS forecasters to focus on other relevant factors. A screenshot of the application is shown in Figure 39.

4. Conclusion

The Rocky Branch Creek watershed in downtown Columbia, South Carolina is prone to significant flash flooding on short time scales during convective heavy rainfall events. This is due to the watershed being highly urbanized with significant steep terrain changes over short distances and a significant stormwater sewer system. Due to the rapid response of the creek to heavy rainfall, FFW decision making by NWS forecasters can be quite challenging. Monitoring rainfall amounts and rates along with potential runoff into the watershed can be complex and time-consuming. To improve the FFW decision making methodology and hopefully extend lead times for these somewhat frequent and significant high-water events during the convective season, two models (using multiple linear regression techniques) were developed to predict the stage heights on the Rocky Branch Creek. One at the upstream stream gauge at Pickens Street (RBPS1) and another at the downstream gauge at Main and Whaley Streets (RBWS1). Since the developmental data sets were relatively small, sufficiently large independent data sets to perform robust verification of the models were not currently available. However, two independent high-water events were examined and the results suggested that the models have forecast skill in predicting the stage heights with the potential to extend warning lead times. It remains important for NWS forecasters to realize the limitations of the models, including that they do not take into account antecedent soil moisture conditions. The FLASH CREST (Coupled Routing and Excess Storage water balance model) soil moisture product in AWIPS, which incorporates antecedent conditions, may be helpful to NWS forecasters in assessing soil moisture conditions prior to convection developing in the watershed (Gourley, et al. 2017). This product used in conjunction with the statistical models may lead to a more accurate estimation of the hydrologic response time. A more robust verification is planned in the future as more independent cases are examined. Furthermore, as more cases are added to the developmental data sets, re-derivation of the models is planned. Additional potential predictors will also be considered in future iterations of the models including the rainfall rates from the Woolpert rain gauges, MRMS Quantitative Precipitation Estimate (QPE), FLASH CREST soil moisture, the storm motion

vector, and environmental shear and stability parameters from the RAP model.

Acknowledgements

The authors would like to thank Frank Alsheimer, WFO Columbia SC SOO, Jeff Waldstreicher, and Jordan Rabinowitz from the NWS Eastern Region Scientific Services Division (SSD) for their review and suggestions. The authors would also like to thank Jacob Wimberley, lead meteorologist at WFO Greenville-Spartanburg SC for providing the script to ingest timely observed Woolpert rainfall amounts and duration data into the AWIPS Hydro Database. Also, thanks to Chris Rohrbach, meteorologist at WFO Columbia SC for assistance with the application development and Pierce Larkin, meteorologist at WFO Columbia SC for creating the topographical map of the Rocky Branch watershed. We would also like to thank Michael Long, Water Analysis Team Leader for Woolpert.

Flood report and composite radar graphics were obtained from the Iowa Environmental Mesonet web site: https://mesonet.agron.iastate.edu/. Skew-t graphics were generated from the University of Wyoming web site https://weather.uwyo.edu/upperair/sounding.html

Disclaimer: Reference to any specific commercial products, process, or service by trade name, trademark, manufacturer, or otherwise, does not constitute or imply its recommendation, or favoring by the United States Government or NOAA/National Weather Service. Information from this publication shall not be used for advertising or product endorsement purposes.

References

Benjamin, S.G., and Coauthors, 2016: A North American Hourly Assimilation and Model Forecast Cycle: The Rapid Refresh. *Mon. Wea. Rev.*, **144**, 1669-1694. https://doi.org/10.1175/MWR-D-15-0242.1

Bothwell, P.D., J.A. Hart, and R.L. Thompson, 2002: An integrated three-dimensional objective analysis scheme in use at the Storm Prediction Center. Preprints, *21st Conf. on Severe Local Storms*, San Antonio, TX, Amer. Meteor. Soc., JP3.1.

Chatterjee, S., A.S. Hadi, B. Price, 2000: *Regression Analysis by Example*. 3rd ed. John Wiley and Sons, 359 pp.

Draper, N. R., and H. Smith, 1998: *Applied Regression Analysis*. 3rd ed. John Wiley and Sons, 709 pp.

Filiaggi, M. T., S. B. Smith, M.Churma, L. Xin, and M. Glaudemans, 2002: Flash flood monitoring and prediction version 2.0: Continued AWIPS modernization. *Preprints, 18th Int. Conf. on IIPS for Meteorology, Oceanography, and Hydrology,* Orlando, FL, Amer. Meteor. Soc., J7.7. [Available online at http://ams.confex.com/ams/pdfpapers/28589.pdf]

Gant, C., 2020: Hydroviewer AGOL (V1.1). Accessed 30 March 2023, https://noaa.maps.arcgis.com/apps/dashboards/c6b6620afa4844fe977bc662e63b0949#rfc=ALR

Gourley, J.J., and Coauthors, 2017: The Flash Project Improving the Tools for Flash Flood Monitoring and Prediction across the United States. *Bull. Amer. Meteor. Soc*., **98**, 361-372, https://doi.org/10.1175/BAMS-D-15-00247.1

Helsley, A.J., 2015: *Columbia South Carolina A History*. The History Press, 176 pp.

Morsy, M.M., J.L. Goodall, F.M. Shatnawi, and M.E. Meadows, 2016: Distributed Stormwater Controls for Flood Mitigation within Urbanized Watersheds: Case Study of Rocky Branch Watershed in Columbia, South Carolina. *J. Hydrol. Eng*. **21**, (11), 05016025.

Neter, J., M.H. Kutner, C.J. Nachtsheim, and W. Wasserman, 1996: *Applied Linear Statistical Models*. 4th ed. Times Mirror Higher Education Group, 1408 pp.

Petersen W. A., and Coauthors, 1999: Mesoscale and radar observations of the Fort Collins flash flood of 28 July 1997. *Bull. Amer. Meteor. Soc*, **80**, 191–216. https://doi.org/10.1175/1520-0477(1999)080<0191:MAROOT>2.0.CO;2

R Core Team, 2014: A Language and Environment for Statistical Computing. R Foundation for Statistical Computing, Vienna, Austria. Accessed 29 March 2023, http://www.R-project.org/

Ress, L.D., C.-L.J. Hung, L.A. James, 2020: Impacts of Urban Drainage Systems on Stormwater Hydrology: Rocky Branch Watershed, Columbia, South Carolina. *Journal of Flood Risk Management*, 13 pp., https://onlinelibrary.wiley.com/doi/full/10.1111/jfr3.12643/

Roberts, B., I.L. Jirak, A.J. Clark, S.J. Weiss, and J.S. Kain, 2019: Postprocessing and visualization techniques for convection-allowing ensembles. *Bull. Amer. Meteor. Soc.*, **100**, 1245-1258, https://doi.org/10.1175/BAMS-D-18-0041.1

Smith, S.B., M.T. Filiaggi, M. Churma, J. Roe, M. Glaudemans, R. Erb, and L. Xin, 2008: Flash Flood Monitoring and Prediction in AWIPS Build 5 and Beyond. Accessed 30 March 2023, https://www.nws.noaa.gov/mdl/ffmp/ffmp99AMS.htm

Wickham, H., 2009: *ggplot2 Elegant Graphics for Data Analysis.* Springer New York.

Wilks, D. S., 1995: *Statistical Methods in the Atmospheric Sciences*. Academic Press, 467 pp.

Zhang, J., and Coauthors, 2016: Multi-Radar Multi-Sensor (MRMS) Quantitative Precipitation Estimation: Initial Operating Capabilities. *Bull. Amer. Meteor. Soc.*, **97**, 621–638, https://doi.org/10.1175/BAMS-D-14-00174.1

Figure 1. Graph showing the number of flash flood events in the developmental sample (2017-2022) that occurred along Rocky Branch at the intersection of Whaley Street and Main Street. Flood stage at this location is 7.2 feet.

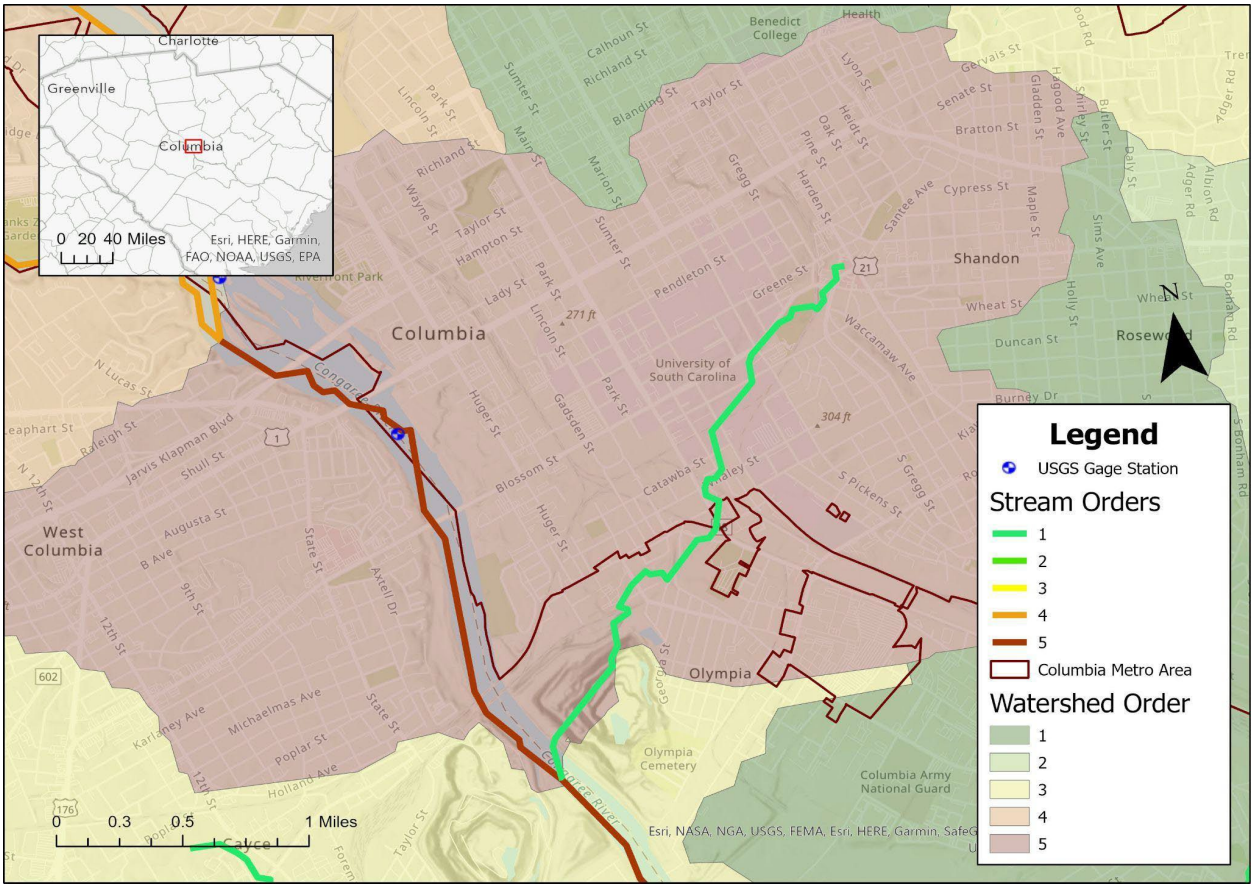

Figure 2. Watersheds of the Columbia metro area within the Saluda river basin. Rocky Branch is shown in light green, flowing into the Congaree River.

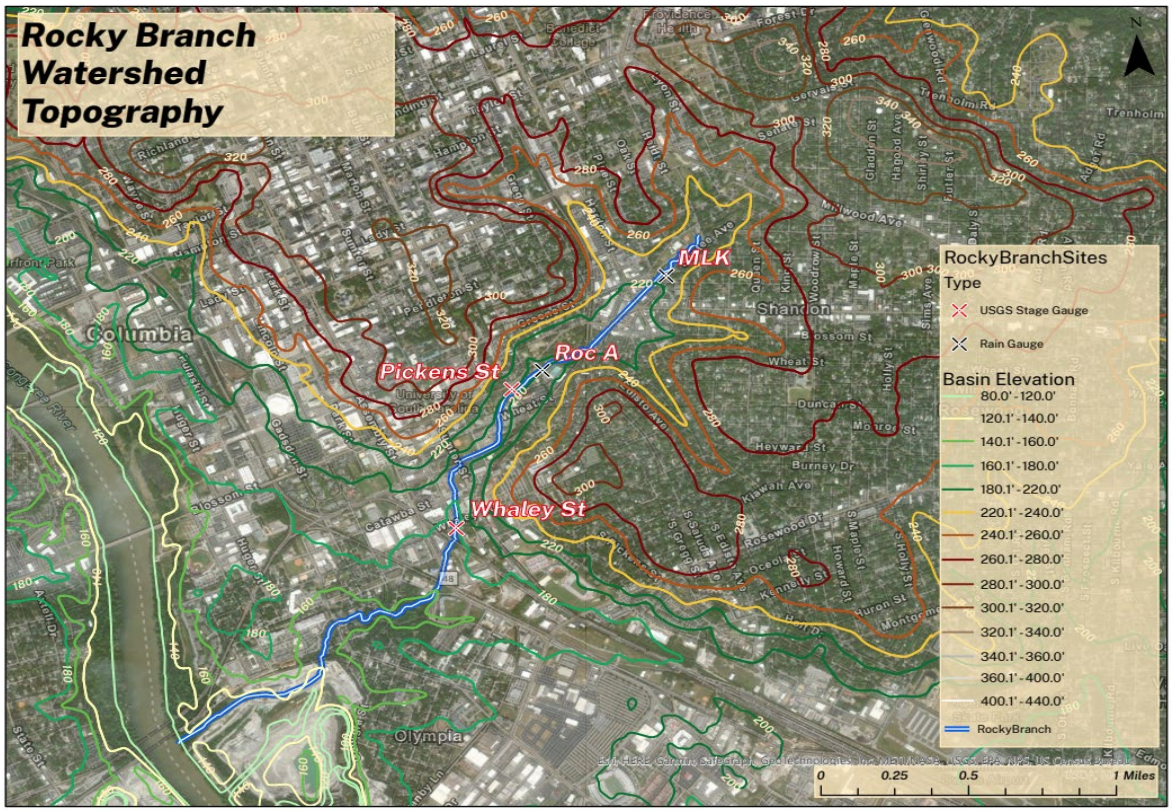

Figure 3. Topographic map of the Rocky Branch Watershed in downtown Columbia, South Carolina.

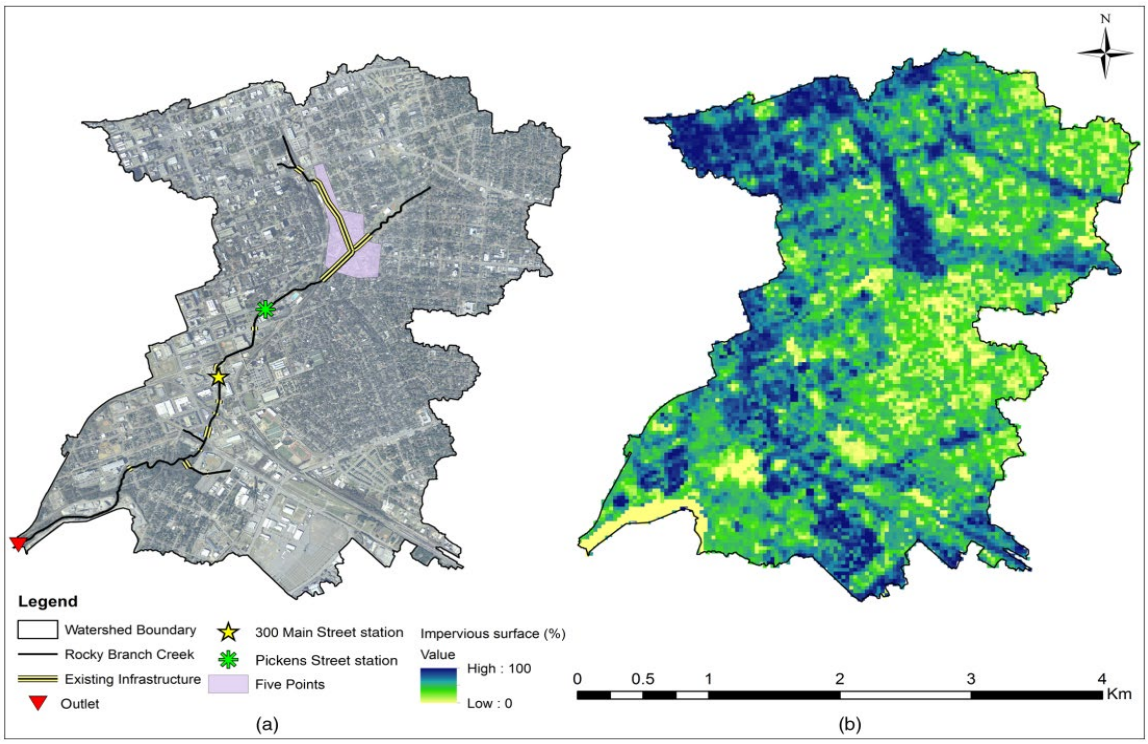

Figure 4. a) Rocky Branch Watershed in downtown Columbia, South Carolina. b) Impervious surfaces according to the National Land Cover Dataset (orthoimagery data from USGS National Map; impervious surface layer data from NLCD 2011). Reprinted with permission from Morsy et al., (2016).

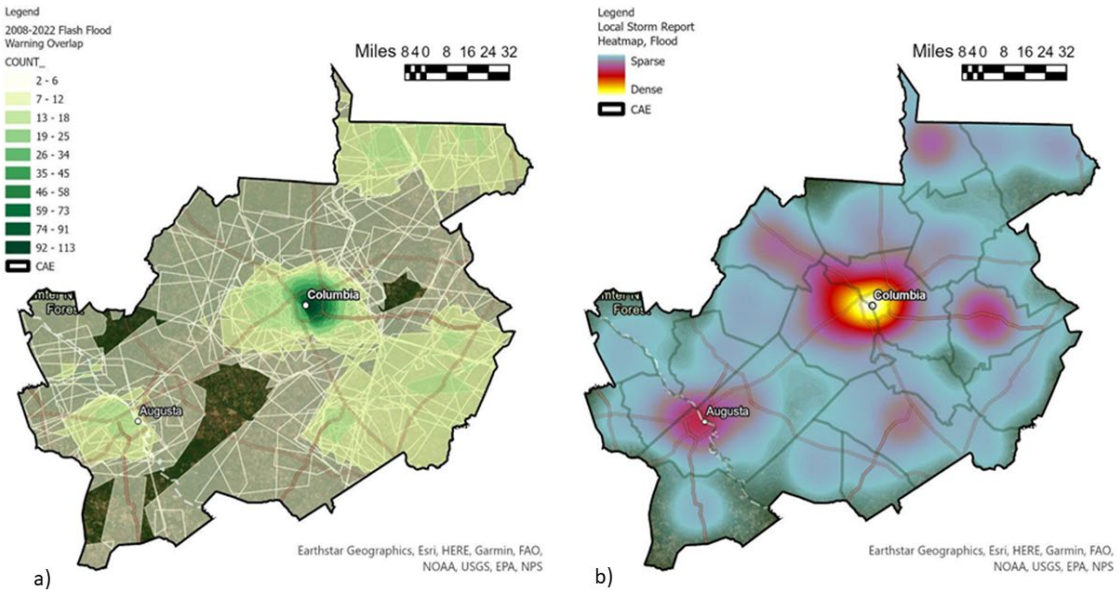

Figure 5. a) Flash Flood Warnings from 2008 to 2022 within the WFO CAE County Warning Area. b) Heat map of Local Storm Reports with Flood tags within the WFO CAE County Warning Area.

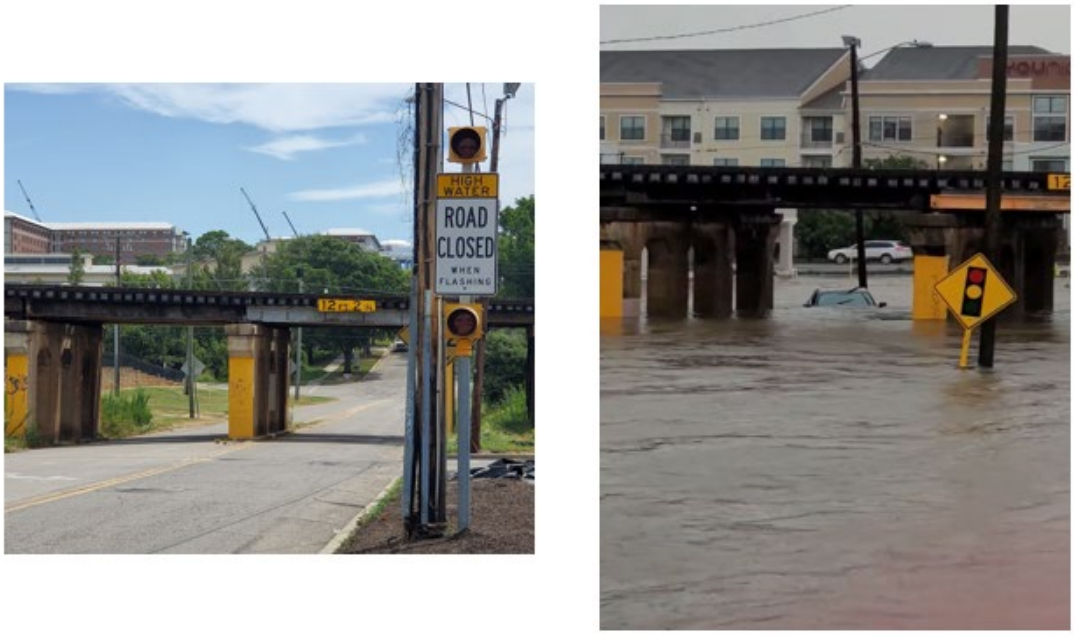

Figure 6. The railroad overpass on Whaley Street near Main Street. When flooding occurs along Rocky Branch this area is significantly impacted. There have been numerous rescues by the Columbia Fire Department extracting people stranded in and on top of their vehicles. The picture of the flooding on the right occurred on 4 July 2022. The stream gauge crested at 12.90 ft. This was the highest crest since the gauge was installed in October 2007.

Figure 7. The intersection of Main Street and Whaley Street. The creek normally flows through a cement culvert underneath the intersection. In the picture, you can see the extensive flooding as the creek flows over the roadway and into the intersection. The flooding picture was taken during the record flood of 4 July 2022.

```
Call:
lm(formula = RBWS1 ~ ROCA + DROCA + MLK + PW)

Residuals:
    Min      1Q  Median      3Q     Max
-2.1802 -0.4914 -0.0614  0.5279  2.3238

Coefficients:
             Estimate Std. Error t value Pr(>|t|)
(Intercept)  5.789278   0.522766  11.074  < 2e-16 ***
ROCA         1.817225   0.429625   4.230 6.11e-05 ***
DROCA       -0.022724   0.004212  -5.395 6.64e-07 ***
MLK          1.495713   0.385600   3.879 0.000213 ***
PW          -0.381846   0.251958  -1.516 0.133536
---
Signif. codes:  0 '***' 0.001 '**' 0.01 '*' 0.05 '.' 0.1 ' ' 1

Residual standard error: 0.7812 on 81 degrees of freedom
Multiple R-squared:  0.8223,    Adjusted R-squared:  0.8136
F-statistic: 93.73 on 4 and 81 DF,  p-value: < 2.2e-16
```

Figure 8. Original model selected to predict the stage height at RBWS1. Note the negative coefficient and high p-value associated with the PW predictor. The PW was determined to be an extraneous variable. The level of statistical significance for each predictor is indicated by the asterisks.

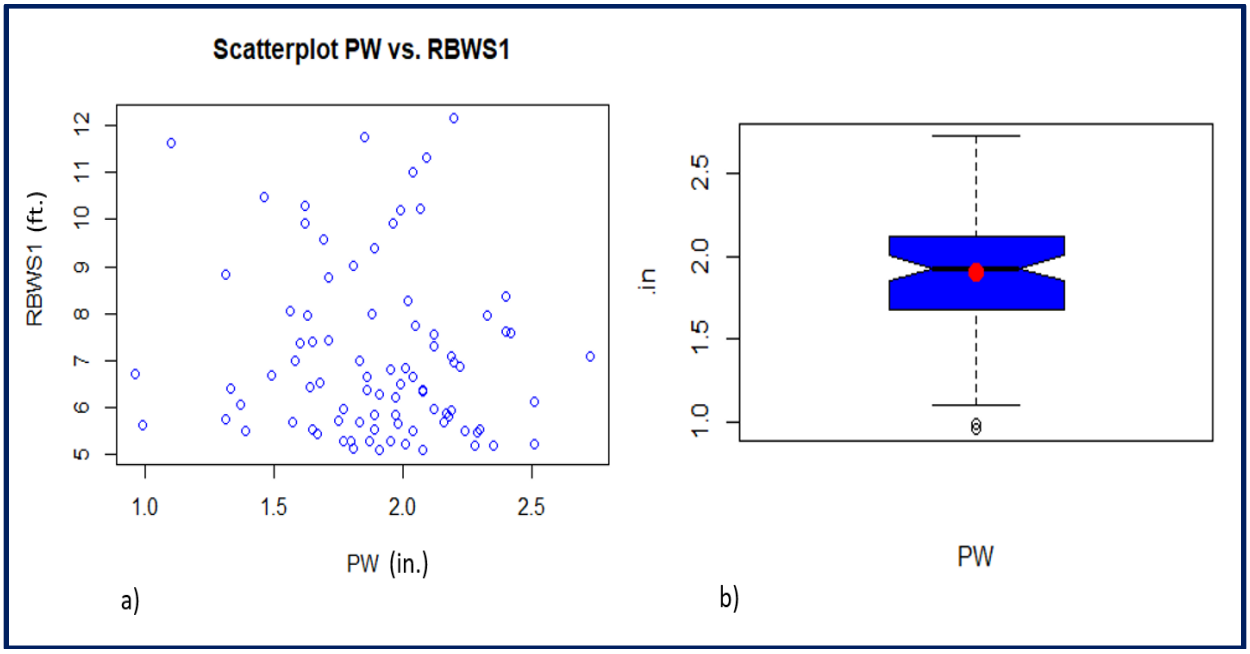

Figure 9. a) Scatter plot of the PW predictor variable vs. the response variable (RBWS1) for the original model RBWS1. PW and RBWS1 do not appear to be well correlated. b) Box and Whisker plot of the PW predictor variable.

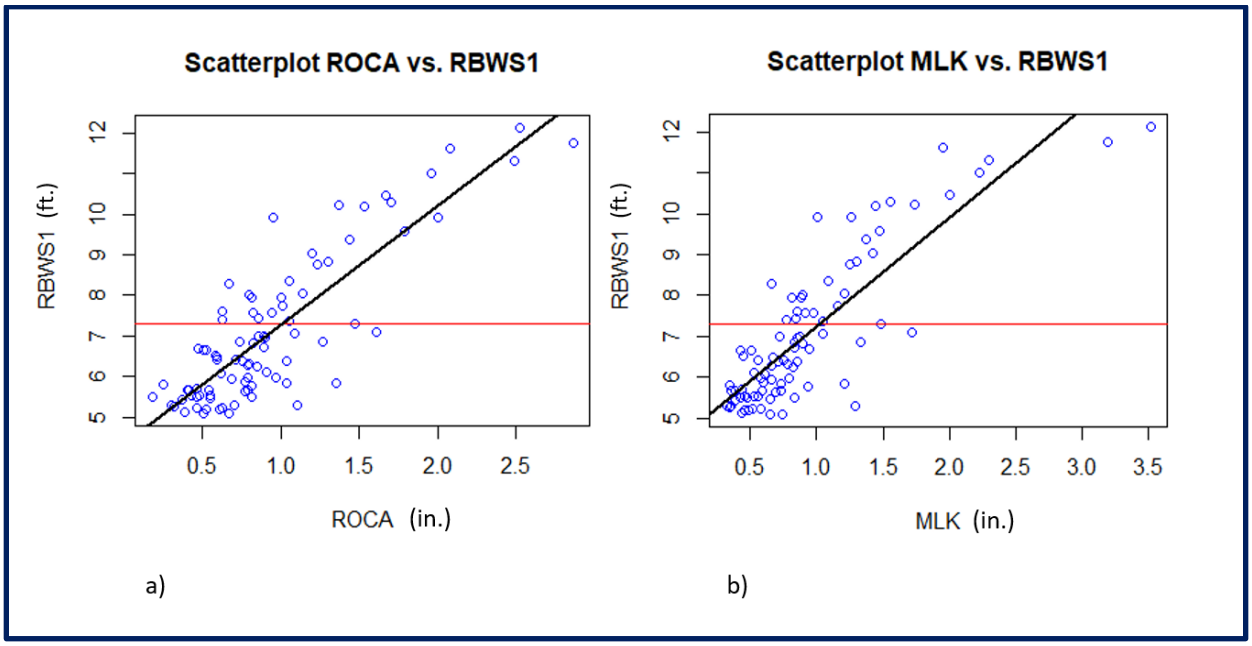

Figure 10. a) Scatter plot of the ROCA rain gauge predictor variable vs. the response variable (RBWS1). The flood stage 7.3 feet is shown in red. The scatter plot suggests rainfall near 1.00 inch at ROCA is associated with flooding. b) Scatter plot of the MLK rain gauge predictor variable vs. the response variable (RBWS1). The flood stage 7.3 feet is shown in red. The scatter plot suggests rainfall near 1.00 inch at MLK is associated with flooding.

```
Call:
lm(formula = RBWS1 ~ ROCA + DROCA + MLK)

Residuals:
     Min       1Q   Median       3Q      Max
-2.17870 -0.52820 -0.00039  0.54778  2.29550

Coefficients:
             Estimate Std. Error t value Pr(>|t|)
(Intercept)  5.068282   0.218390  23.207  < 2e-16 ***
ROCA         1.879719   0.431010   4.361 3.73e-05 ***
DROCA       -0.023158   0.004236  -5.468 4.81e-07 ***
MLK          1.450731   0.387484   3.744 0.000335 ***
---
Signif. codes:
0 '***' 0.001 '**' 0.01 '*' 0.05 '.' 0.1 ' ' 1

Residual standard error: 0.7873 on 82 degrees of freedom
Multiple R-squared:  0.8173,    Adjusted R-squared:  0.8106
F-statistic: 122.3 on 3 and 82 DF,  p-value: < 2.2e-16
```

Figure 11. RBWS1 multiple linear regression model with ROCA, DROCA, and MLK as predictors. The level of statistical significance for each predictor is indicated by the asterisks.

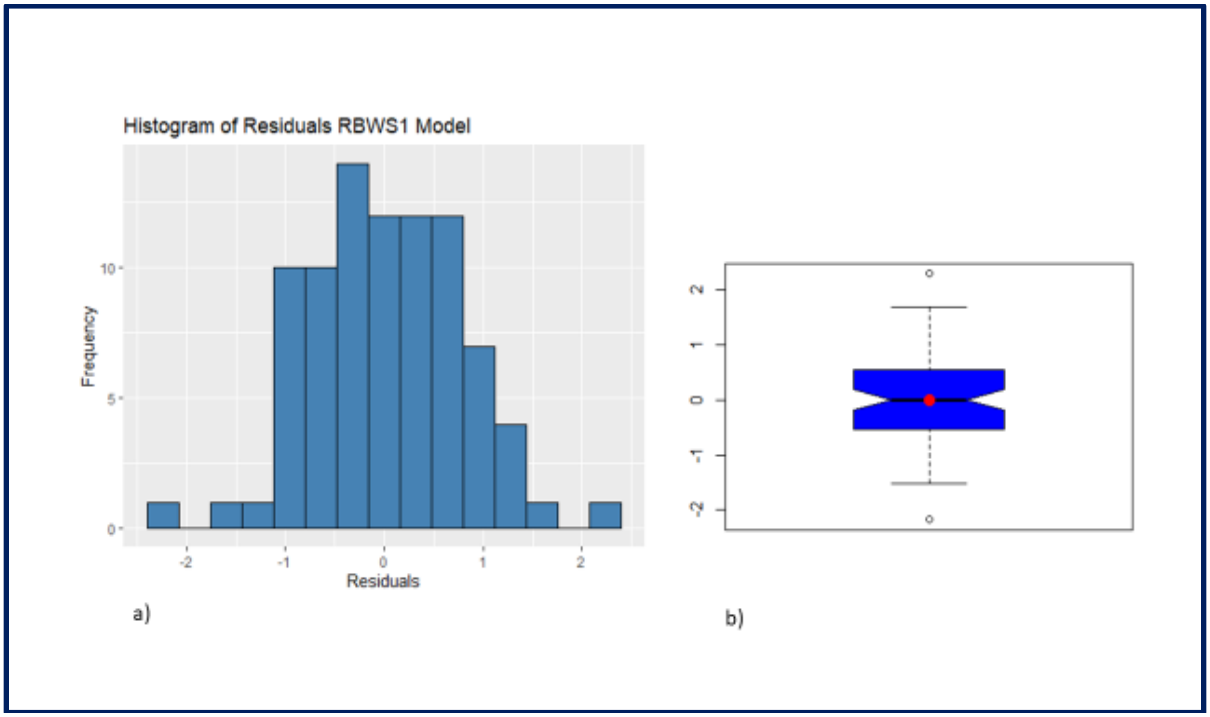

Figure 12. a) Histogram and b) Box and Whisker plot of residuals RBWS1 multiple linear regression model with ROCA, DROCA, and MLK as predictors. The distribution appears near symmetrical although there are outliers with positive kurtosis.

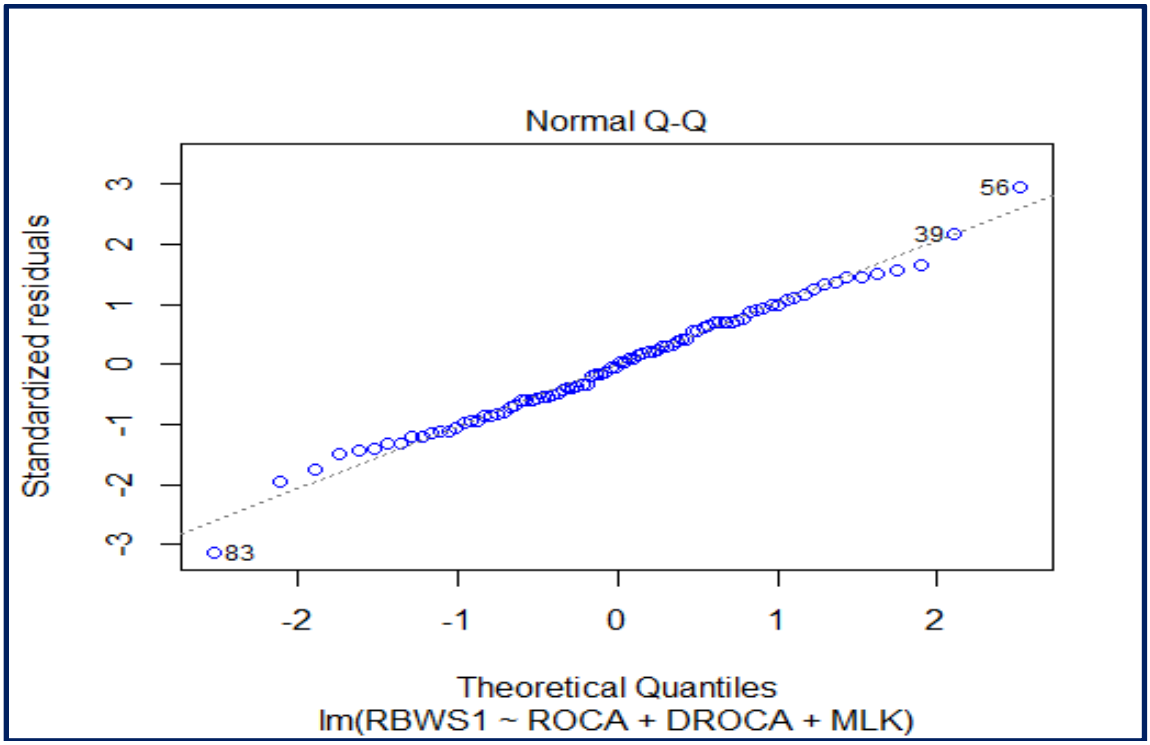

Figure 13. RBWS1 Quantile-Quantile (QQ) plot of the residuals for the selected multiple linear regression model with ROCA, DROCA, and MLK as predictors. Note the distribution of the residuals appears to follow the Gaussian distribution although there are outliers.

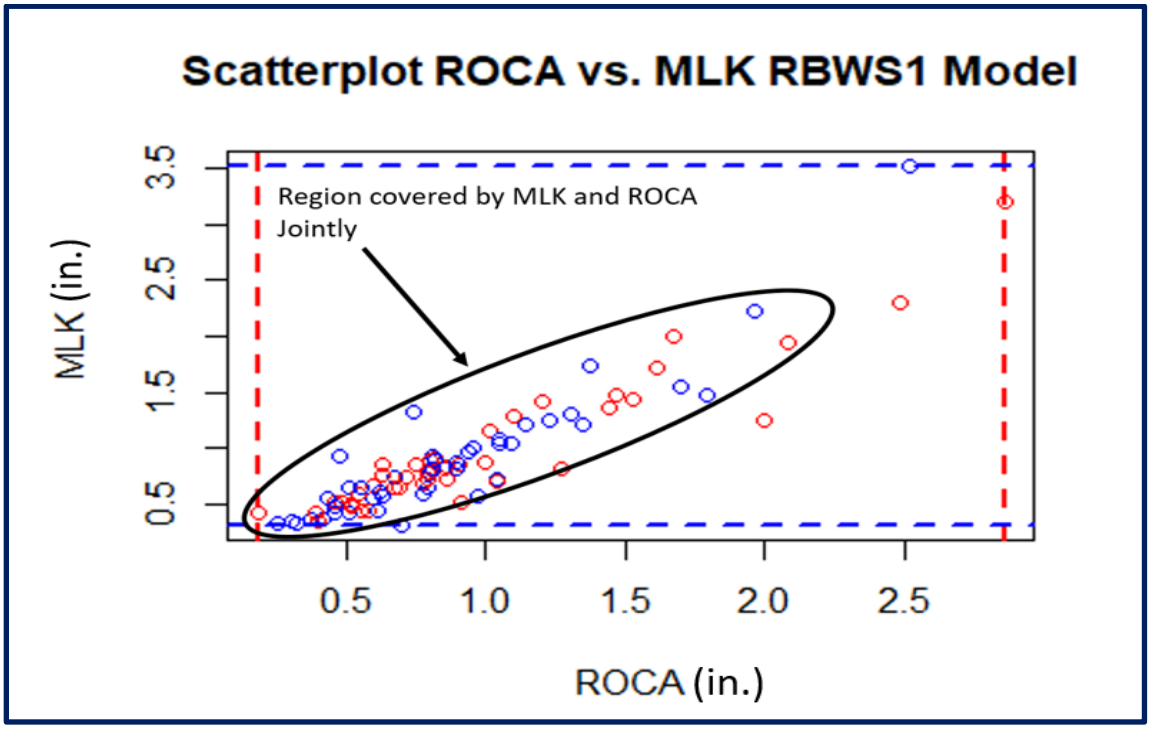

Figure 14. Scatter plot of the ROCA (red dots) and MLK (blue dots) predictor variables for RBWS1 model showing the overlap of observations. Red dashed lines represent the range of values for ROCA. Blue dashed lines represent the range of values for MLK. Most of the observations do not fall outside the overall scope of the model. Note: This is a simplified depiction since DROCA is also a predictor.

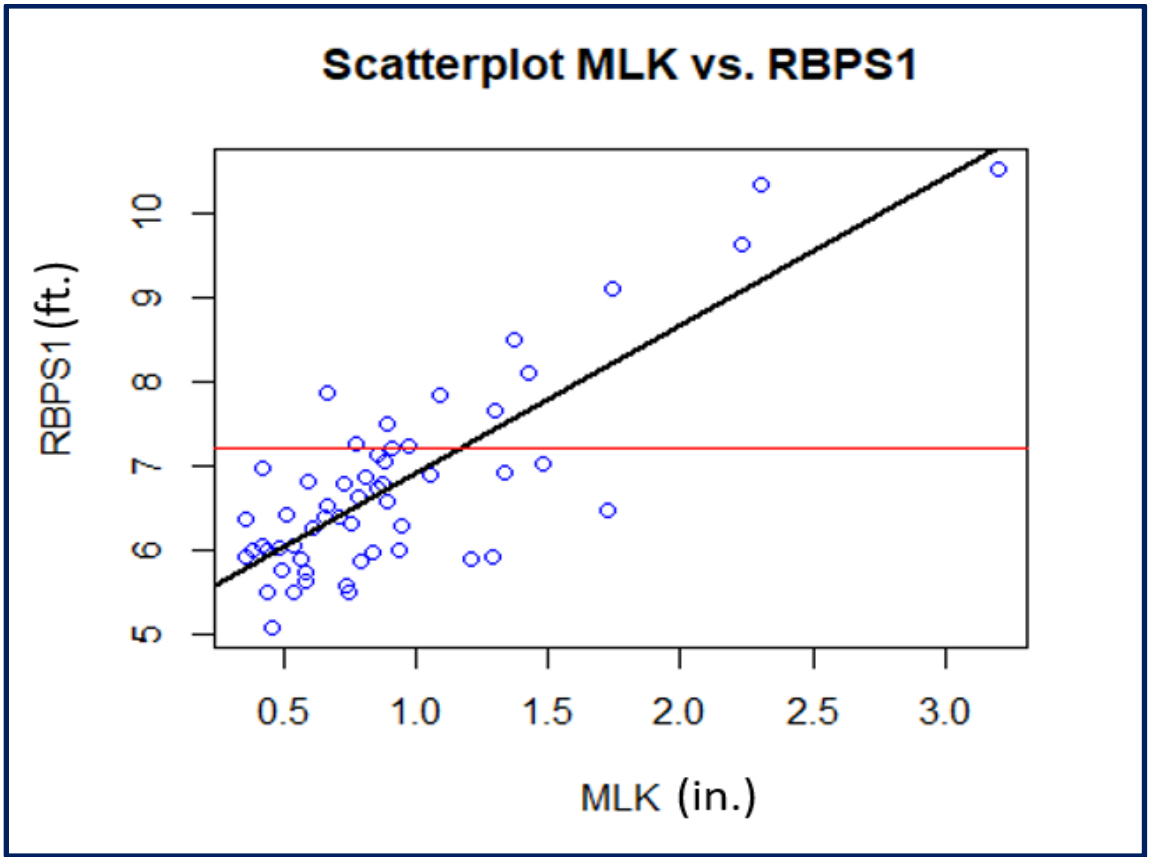

Figure 15. Scatter plot of the MLK rain gauge predictor variable vs. the response variable (RBPS1). The flood stage 7.2 feet is shown in red. The scatter plot suggests rainfall near 1.20 inches at MLK is associated with flooding.

```
Call:
lm(formula = RBPS1 ~ MLK + DMLK, data = dat4)

Residuals:
     Min       1Q   Median       3Q      Max
-1.08235 -0.24981  0.07586  0.23509  1.00588

Coefficients:
             Estimate Std. Error t value Pr(>|t|)
(Intercept)  5.537181   0.153566  36.057  < 2e-16 ***
MLK          2.410524   0.154592  15.593  < 2e-16 ***
DMLK        -0.019183   0.002671  -7.181 3.48e-09 ***
---
Signif. codes:  0 ‘***’ 0.001 ‘**’ 0.01 ‘*’ 0.05 ‘.’ 0.1 ‘ ’ 1

Residual standard error: 0.4359 on 49 degrees of freedom
Multiple R-squared:  0.8325,    Adjusted R-squared:  0.8257
F-statistic: 121.8 on 2 and 49 DF,  p-value: < 2.2e-16
```

Figure 16. RBPS1 multiple linear regression model with MLK and DMLK as predictors. The level of statistical significance for each predictor is indicated by the asterisks.

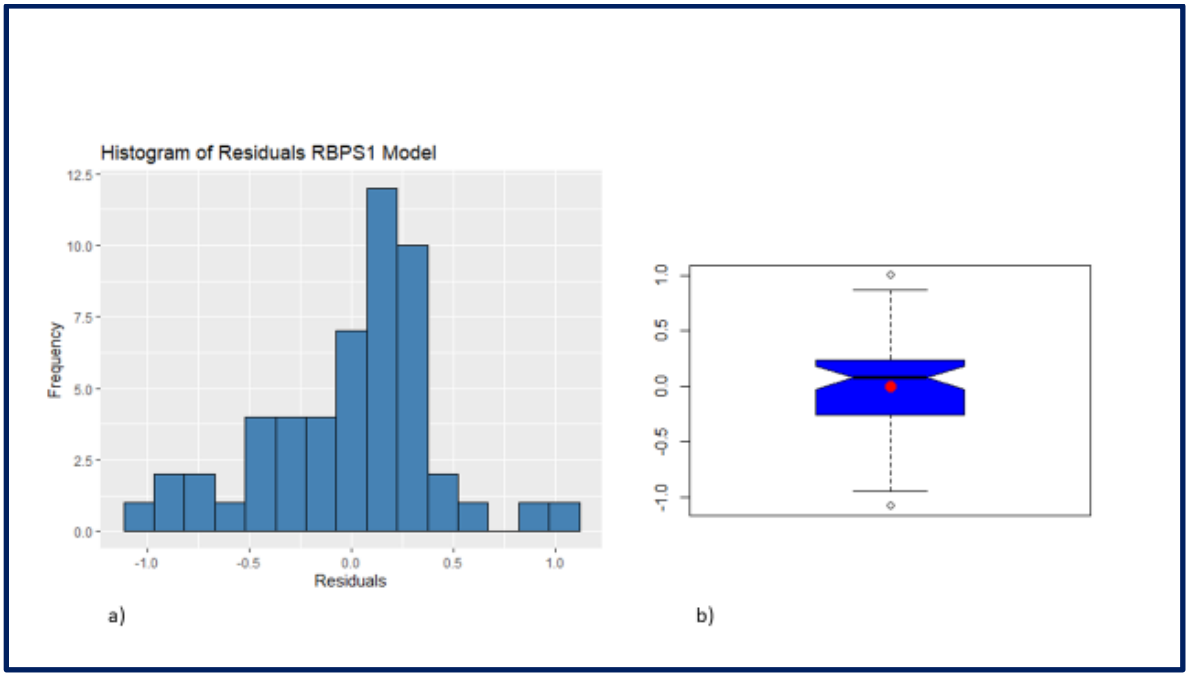

Figure 17. a) Histogram and b) Box and Whisker plot of residuals RBPS1 multiple linear regression model with MLK and MLKD as predictors. The distribution appears left-skewed (negative) with outliers.

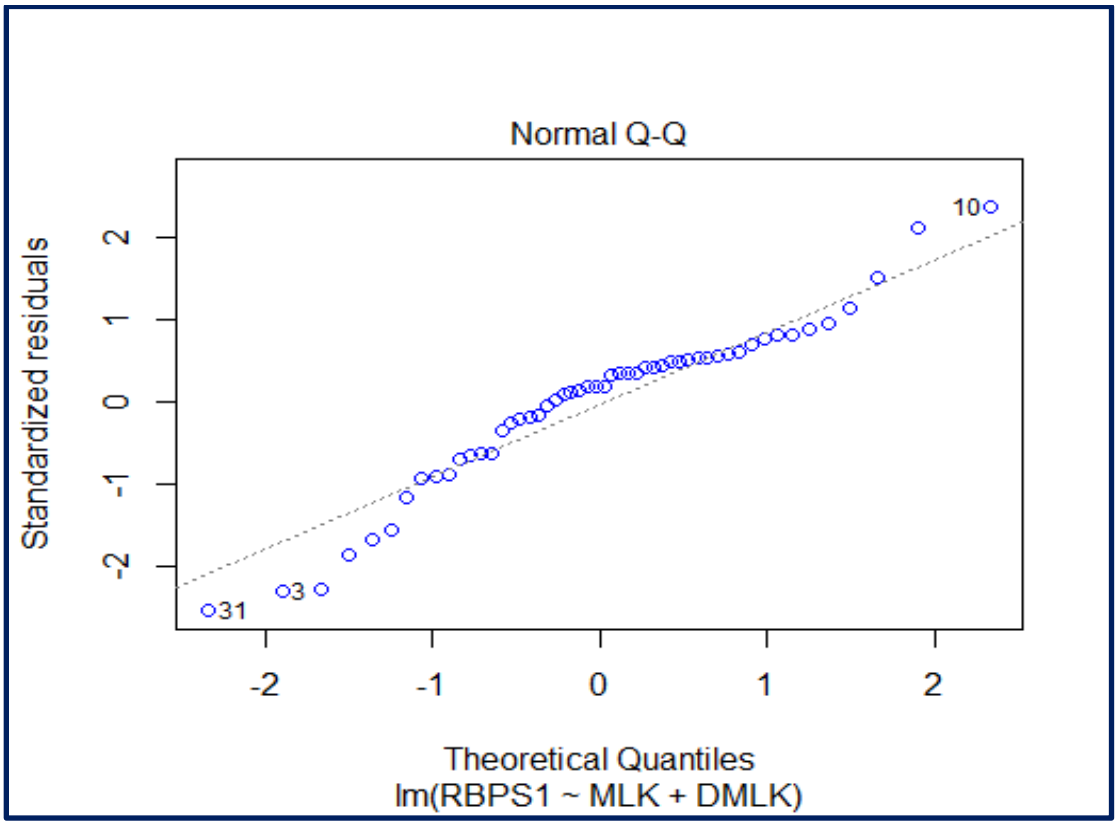

Figure 18. RBPS1 Quantile-Quantile (QQ) plot of the residuals for the multiple linear regression model with MLK and DMLK as predictors. Note the distribution of the residuals appears to be left-skewed (negative) with a heavy left tail.

```
Call:
lm(formula = RBPS1 ~ MLK + DMLK, data = dat7)

Residuals:
    Min      1Q  Median      3Q     Max
-11.100  -2.156   1.068   3.287  10.990

Coefficients:
            Estimate Std. Error t value Pr(>|t|)
(Intercept) 25.03815    1.99155   12.57  < 2e-16 ***
MLK         38.03702    1.88843   20.14  < 2e-16 ***
DMLK        -0.24669    0.03403   -7.25 3.42e-09 ***
---
Signif. codes:  0 '***' 0.001 '**' 0.01 '*' 0.05 '.' 0.1 ' ' 1

Residual standard error: 5.243 on 47 degrees of freedom
Multiple R-squared:  0.8962,    Adjusted R-squared:  0.8918
F-statistic: 202.9 on 2 and 47 DF,  p-value: < 2.2e-16
```

Figure 19. RBPS1A multiple linear regression model with MLK and DMLK as predictors. The level of statistical significance for each predictor is indicated by the asterisks. Note the low p-values indicating statistically significance and higher adjusted R^2 than the RBPS1 equation.

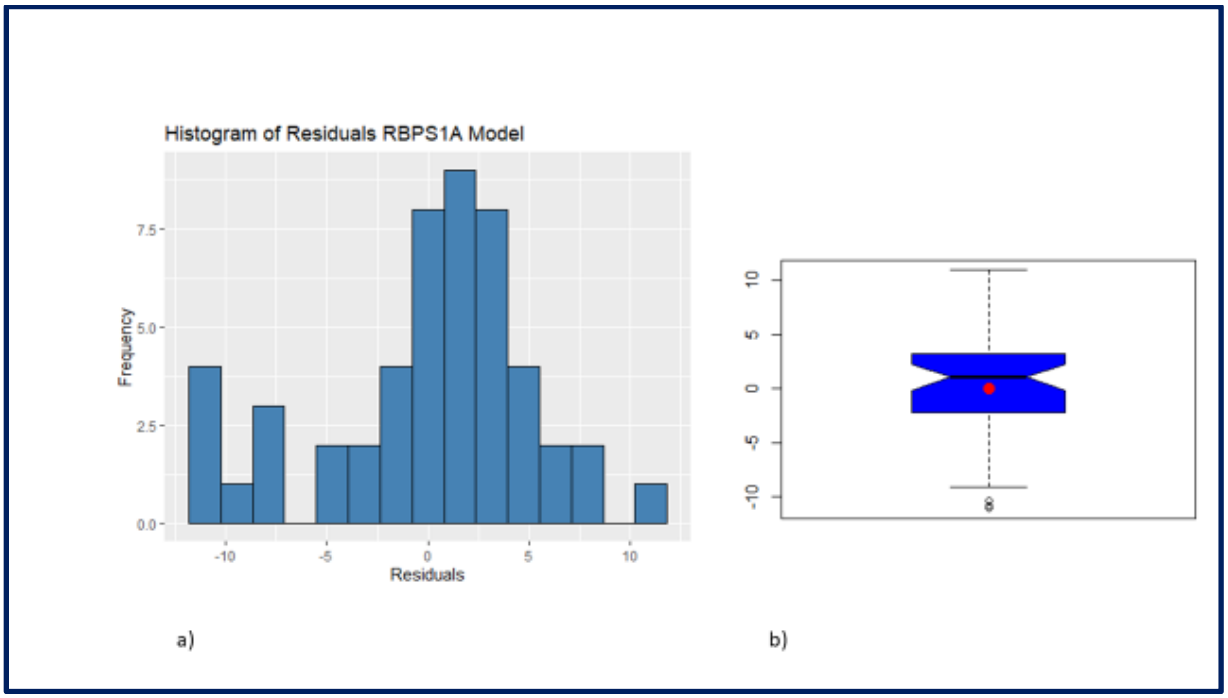

Figure 20. a) Histogram and b) Box and Whisker plot of residuals RBPS1A multiple linear regression model with MLK and MLKD as predictors. The distribution still appears left-skewed (negative) with outliers but closer to a normal distribution than RBPS1 after the transformation.

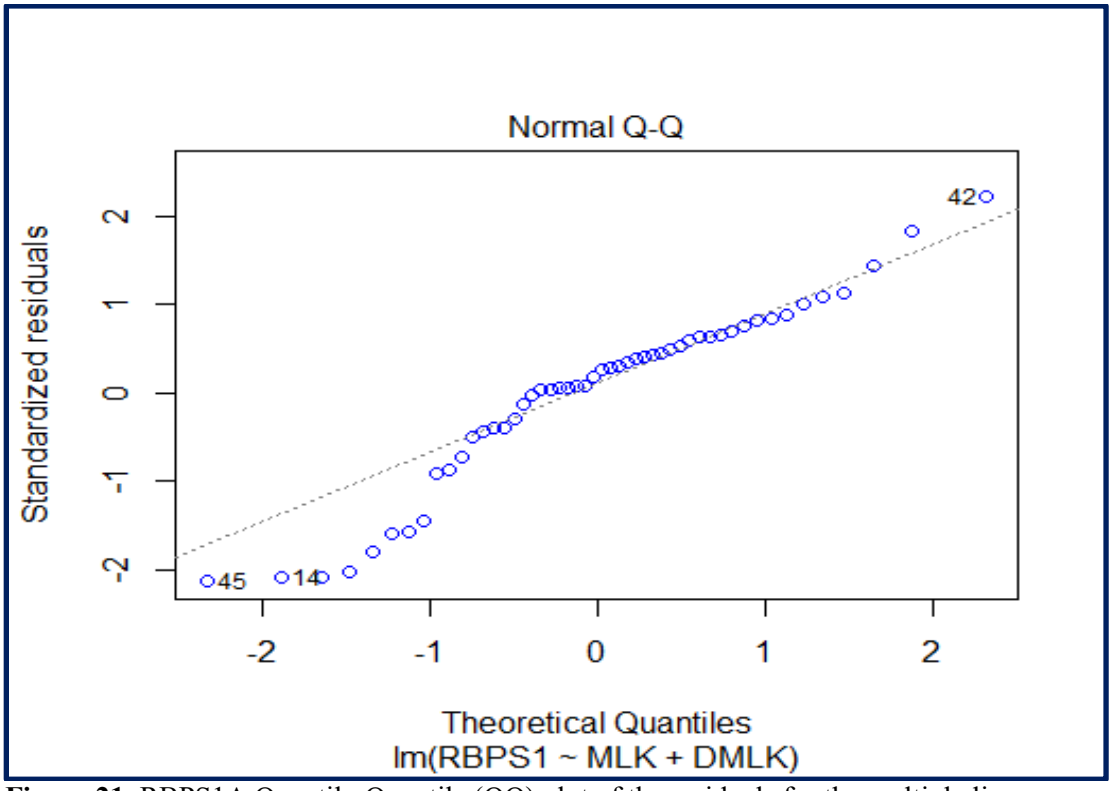

Figure 21. RBPS1A Quantile-Quantile (QQ) plot of the residuals for the multiple linear regression model with MLK and MLKD as predictors. Note the distribution of the residuals appears to still be left-skewed (negative) with a heavy left tail although the predicted values appear reasonable to the theoretical. The transformed RBPS1A was chosen as the equation RBPS1.

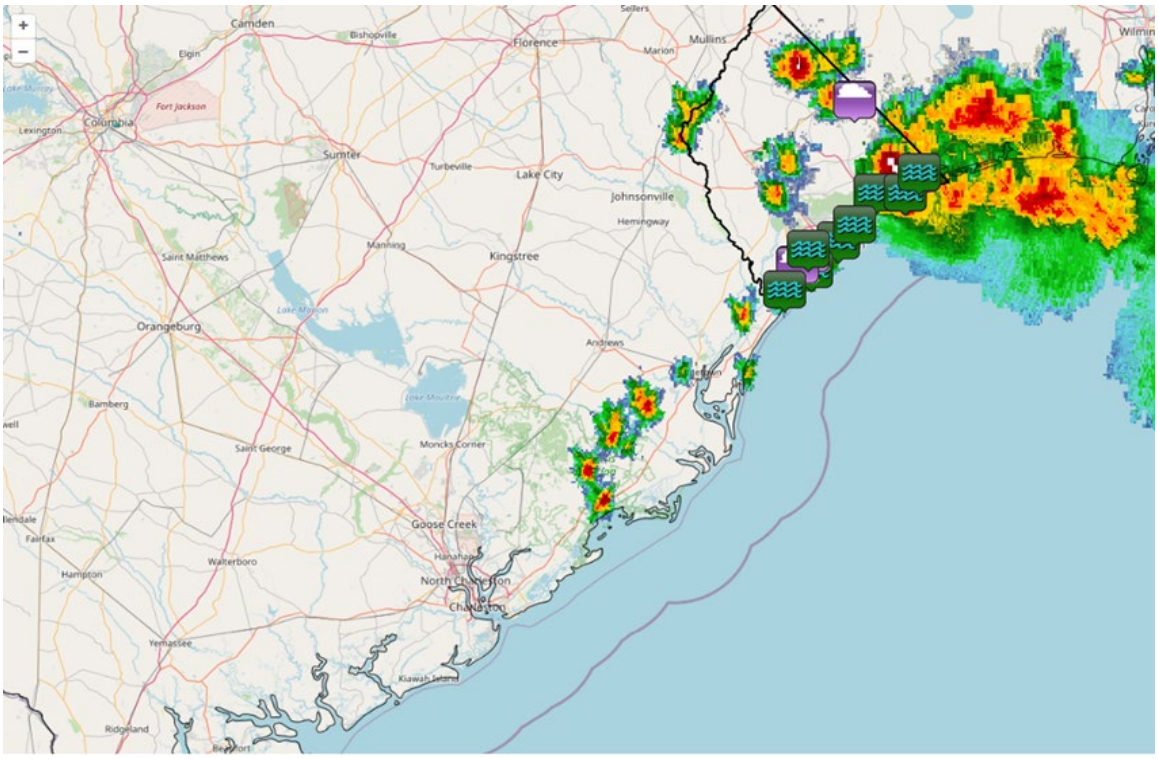

Figure 22. Flash Flooding reports and Radar Composite Reflectivity valid 1545 UTC 4 July 2022.

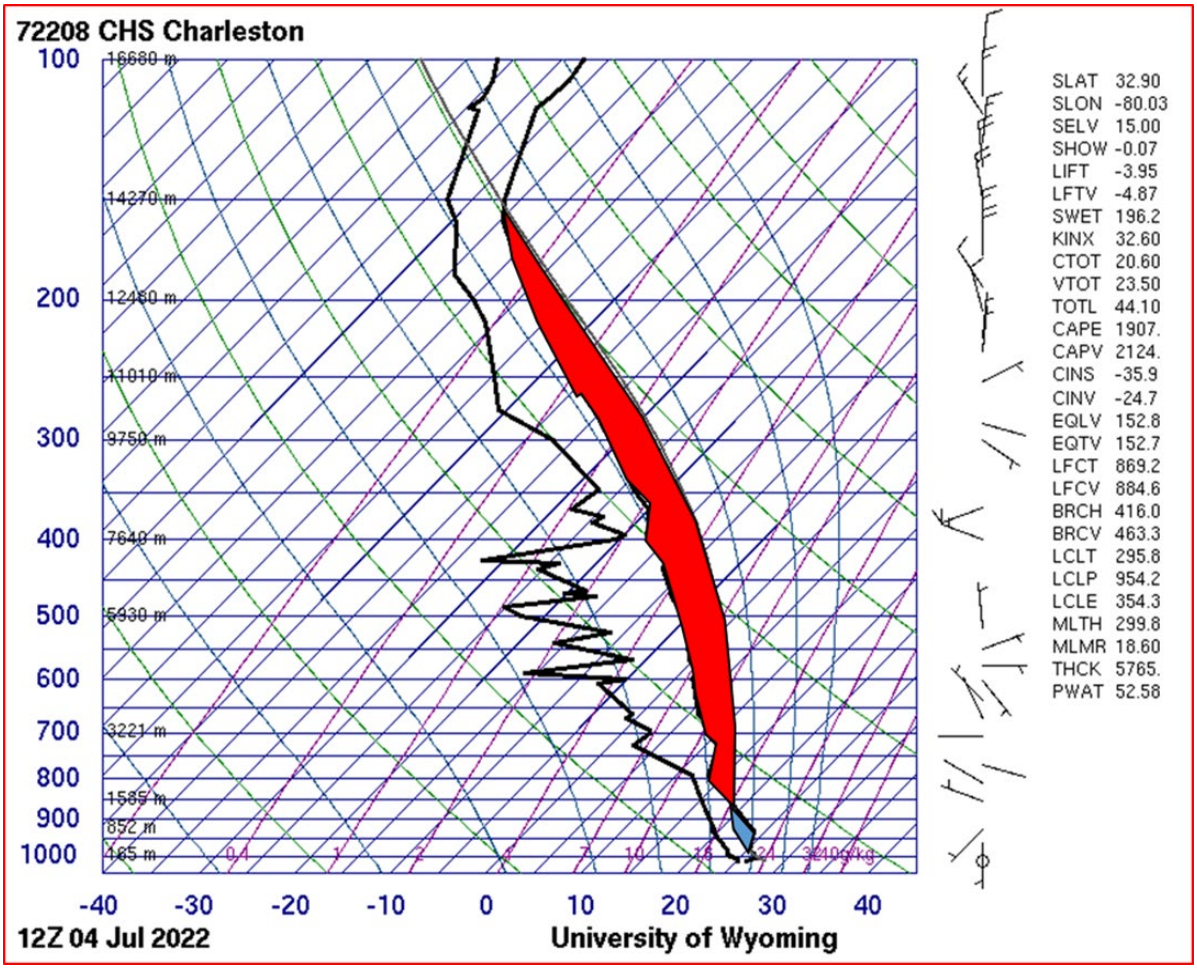

Figure 23. RAOB sounding at CHS valid 1200 UTC 4 July.

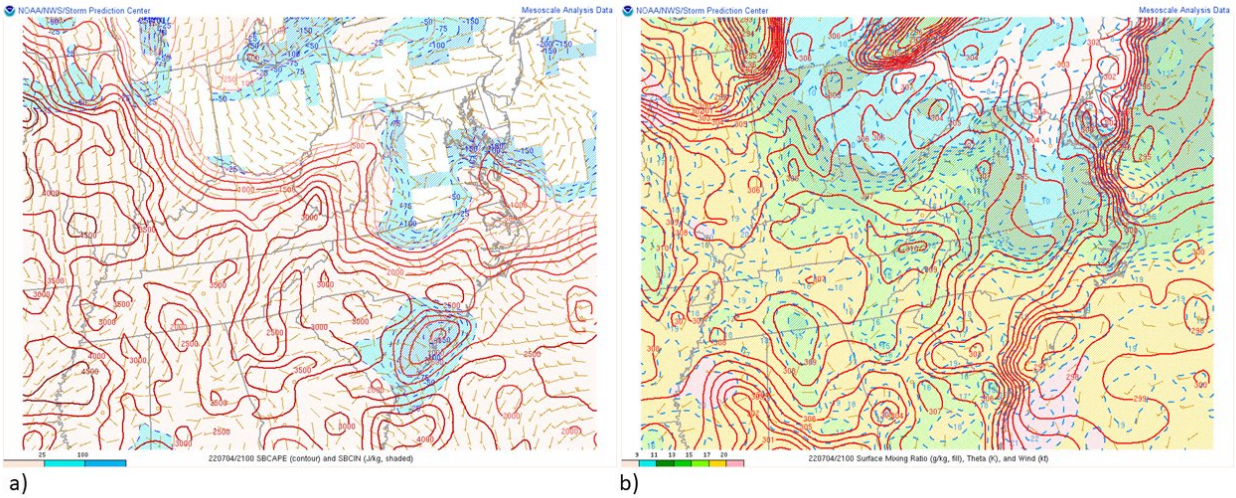

a) b)

Figure 24. SPC mesoanalysis of a) Surface-based Convective Potential Energy (CAPE), Surface-based Convective Inhibition (CIN) J/kg, and Wind (kt.) valid 2100 UTC 4 July 2022. b) Surface Mixing Ratio g/kg, fill), Theta (K), and Wind (kt.) valid 2100 UTC 4 July 2022.

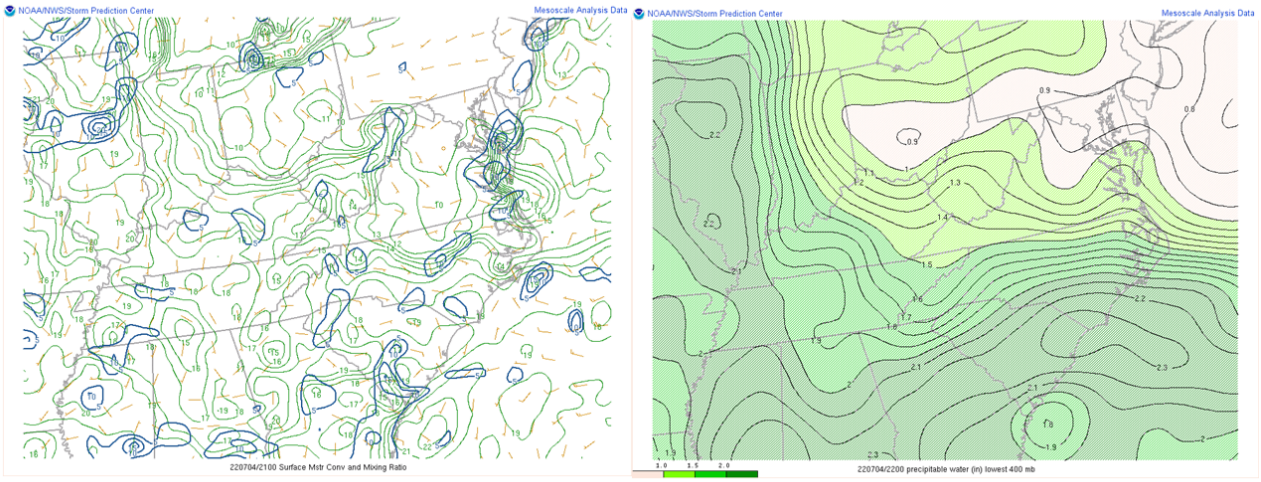

a) b)

Figure 25. SPC mesoanalysis of a) Surface Moisture Convergence, Mixing Ratio g/kg, Wind (kt.) valid 2100 UTC 4 July 2022. b) Precipitable Water (in.) valid 2100 UTC 4 July 2022.

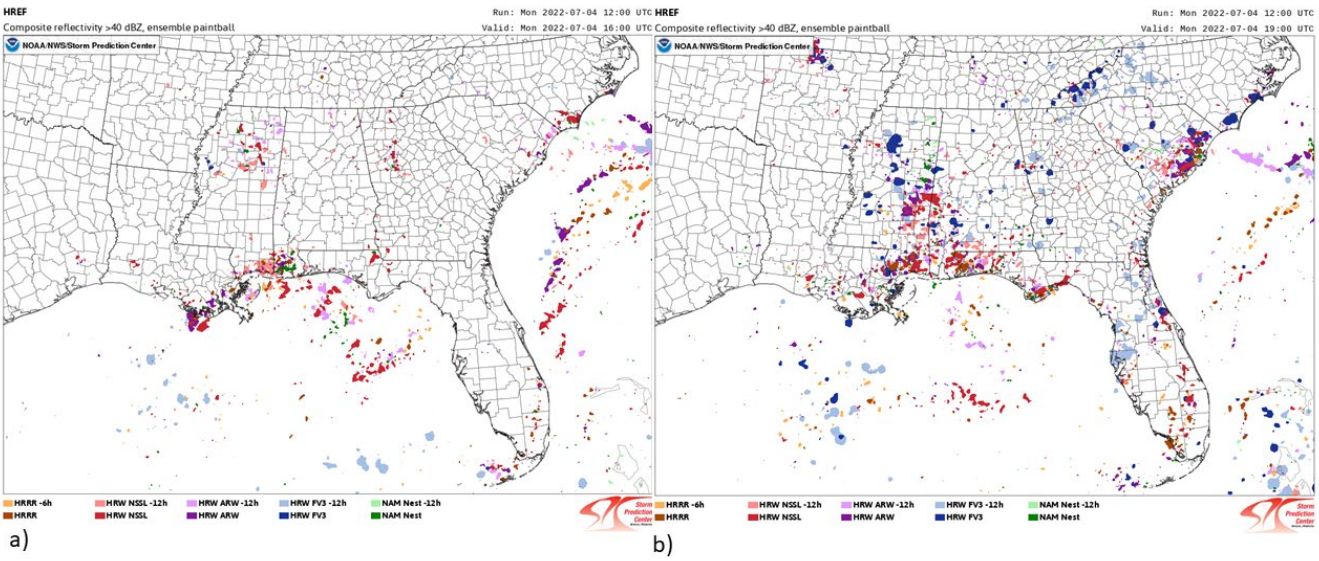

a) b)

Figure 26. a) 1200 UTC 4 July 2022 run HREF Composite Reflectivity > 40 dBZ, ensemble paintball valid 1600 UTC 4 July 2022. b) 1200 UTC 4 July 2022 run HREF Composite Reflectivity > 40 dBZ, ensemble paintball valid 1900 UTC 4 July 2022.

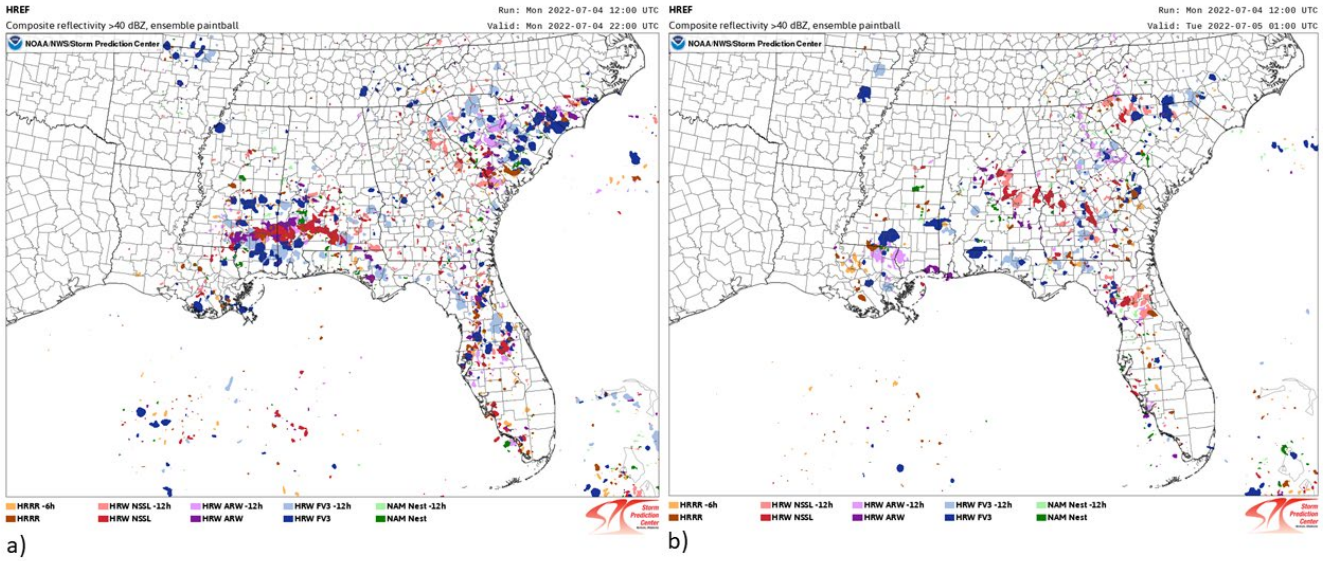

Figure 27. a) 1200 UTC 4 July 2022 run HREF Composite Reflectivity > 40 dBZ, ensemble paintball valid 2200 UTC 4 July 2022. b) 1200 UTC 4 July 2022 run HREF Composite Reflectivity > 40 dBZ, ensemble paintball valid 0100 UTC 5 July 2022.

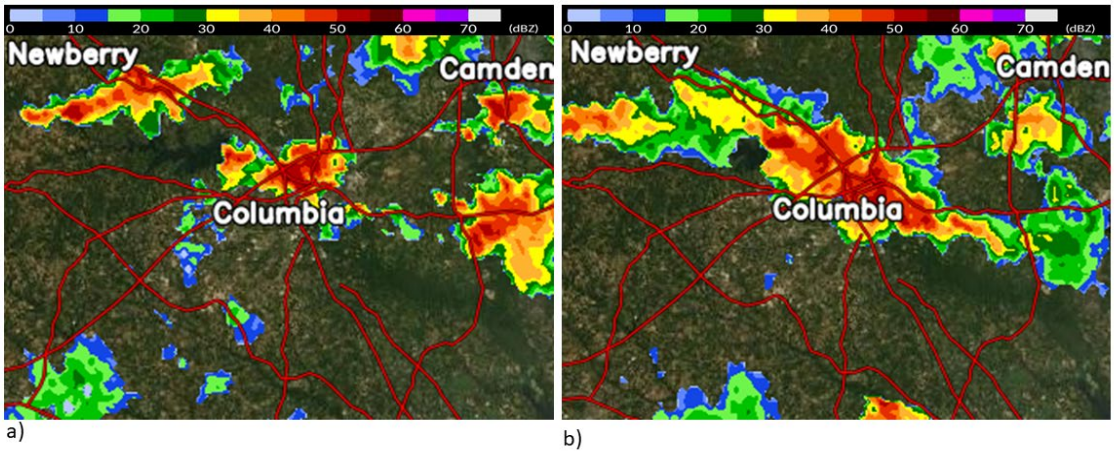

Figure 28. a) MRMS Radar Reflectivity (lowest scan) valid 2130 UTC 4 July 2022.
b) MRMS Radar Reflectivity (lowest scan) valid 2200 UTC 4 July 2022.

TIME(UTC)	ROCA(in.)	MLK(in.)	RBWS1(ft.)	RBPS1(ft.)
2125	0.00	0.03	5.11	5.12
2130	0.01	0.18	5.28	5.64
2135	**0.09**	**0.20**	**5.62**	**6.18**
2140	0.14	0.33	6.25	7.03
2145	0.40	0.53	7.65	8.27
2150	**0.70**	**0.68**	**9.84**	**9.65**
2155	0.92	0.70	12.47	10.88
2200	0.69	0.48	14.34	11.64
2205	0.35	0.42	15.50	12.26
2210	0.51	0.57	17.16	13.06
2215	0.33	0.27	18.06	13.40
2220	0.17	0.15	18.48	13.57
2225	0.09	0.07	18.64	13.62
2230	0.08	0.08	**18.79**	13.69
2235	0.03	0.04	**18.79**	**13.70**
2240	0.03	0.01	18.74	13.67
2245	0.01	0.00	18.64	13.62

Table 1. 4 July 2022 Rocky Branch flash flood case. Woolpert 5 min. rainfall data at ROCA and MLK along with model stage height forecasts for RBWS1 and RBPS1. Decision time to issue a warning based on the models in red. Crest height forecast in purple. Actual Flash Flood Warning issue time in yellow.

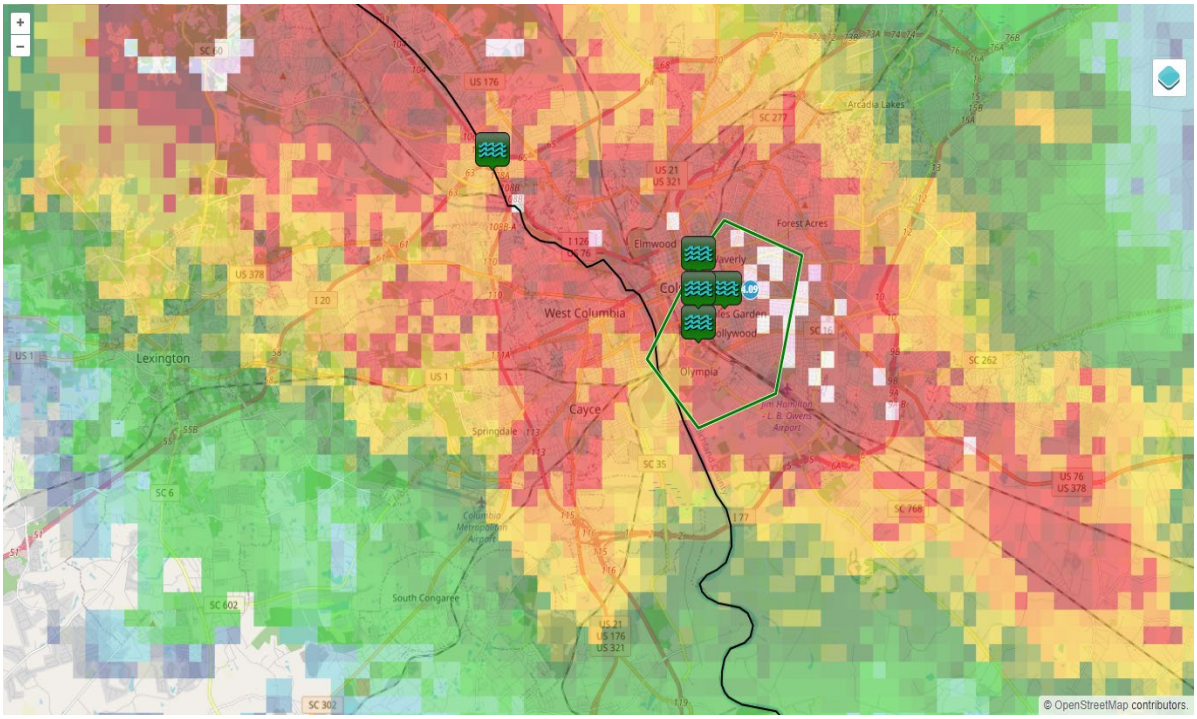

Figure 29. Radar Composite at Flash Flood Warning Issuance Time valid 2150 UTC 4 July 2022 with flash flooding reports.

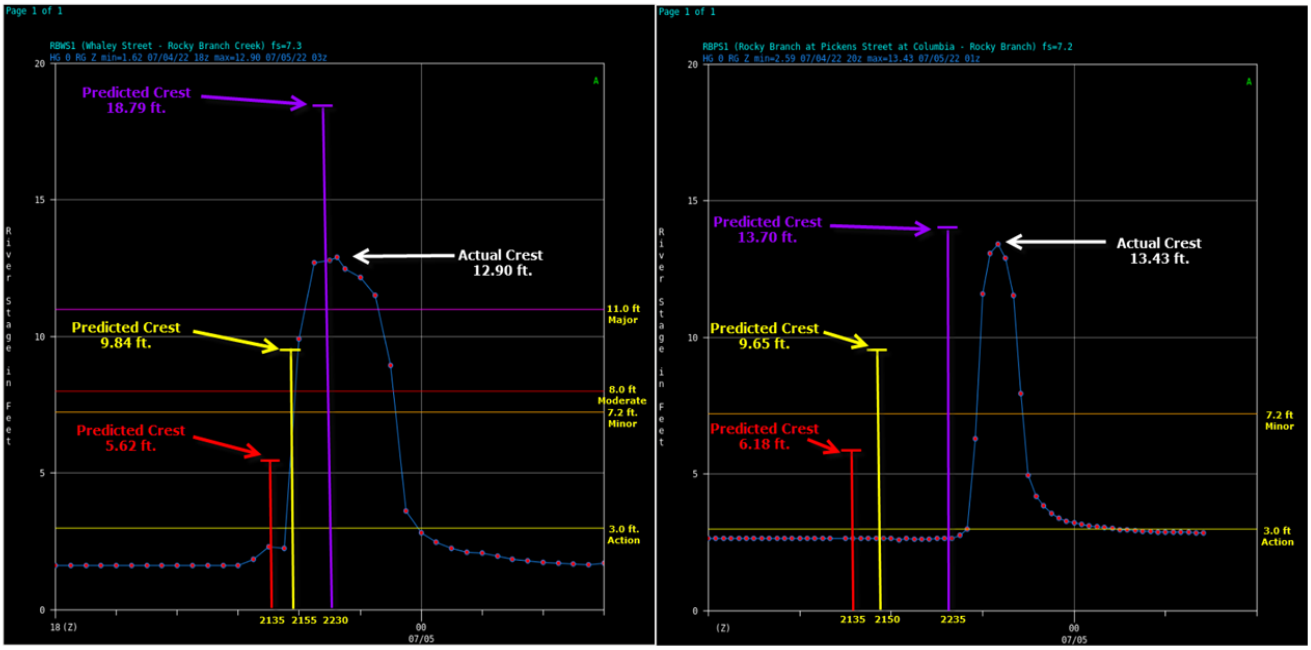

a) b)

Figure 30. a) 4 July 2022 Observed hydrograph at Whaley Street (RBWS1) with model crest forecast and times. Reasonable earliest time a flash flood warning could have been issued based on model output is denoted by the red-colored line. The flash flood warning issued time is denoted by the yellow-colored line, the time of maximum predicted crest is denoted by the purple-colored line, and the actual crest is denoted by the white arrow. b) 4 July 2022 Observed hydrograph at Pickens Street (RBPS1) with model crest forecast and times. Reasonable earliest time a flash flood warning could have been issued based on model output is denoted by the red-colored line. The flash flood warning issued time is denoted by the yellow-colored line, the time of maximum predicted crest is denoted by the purple-colored line, and the actual crest is denoted by the white arrow.

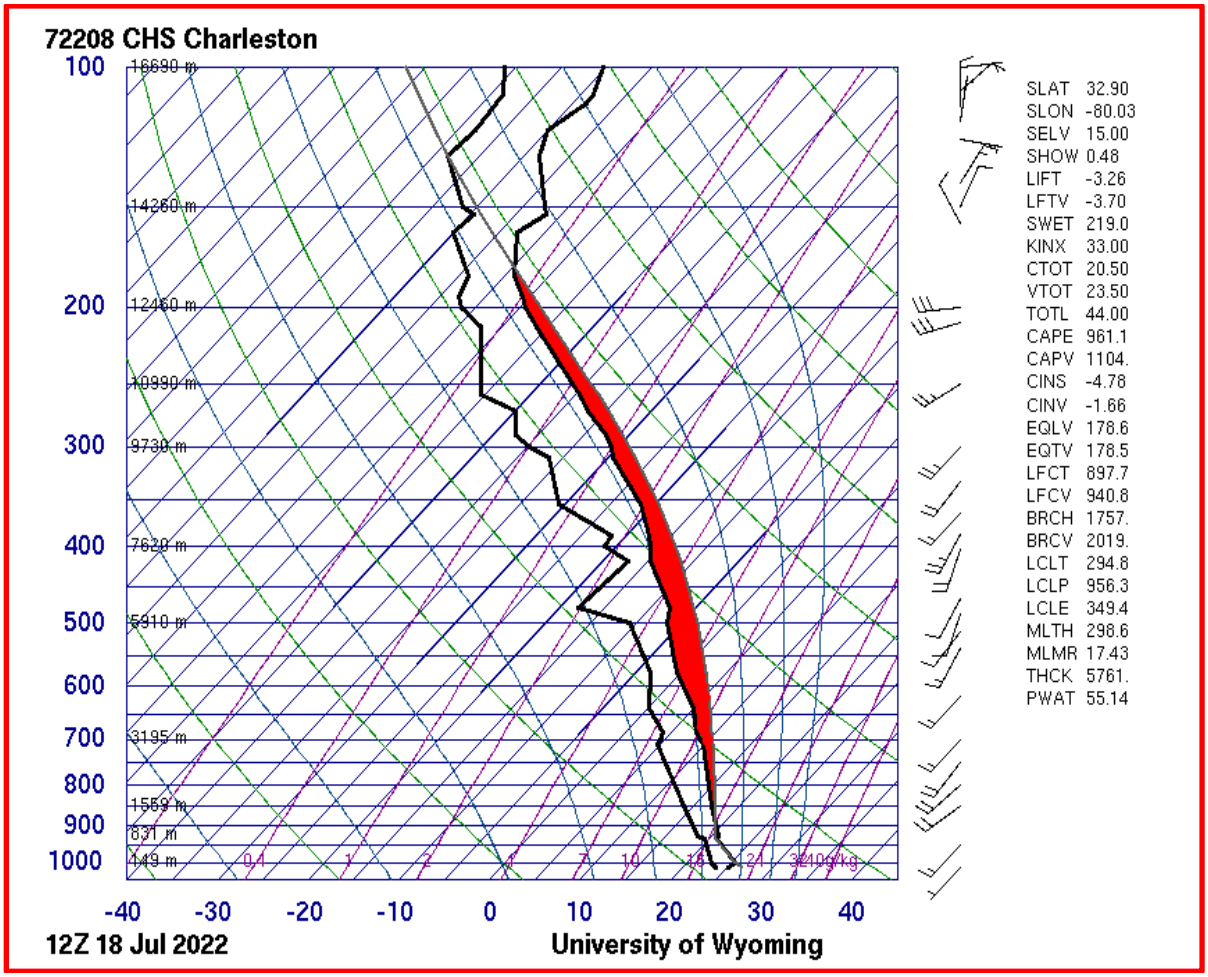

Figure 31. RAOB sounding at CHS valid 1200 UTC 18 July 2022.

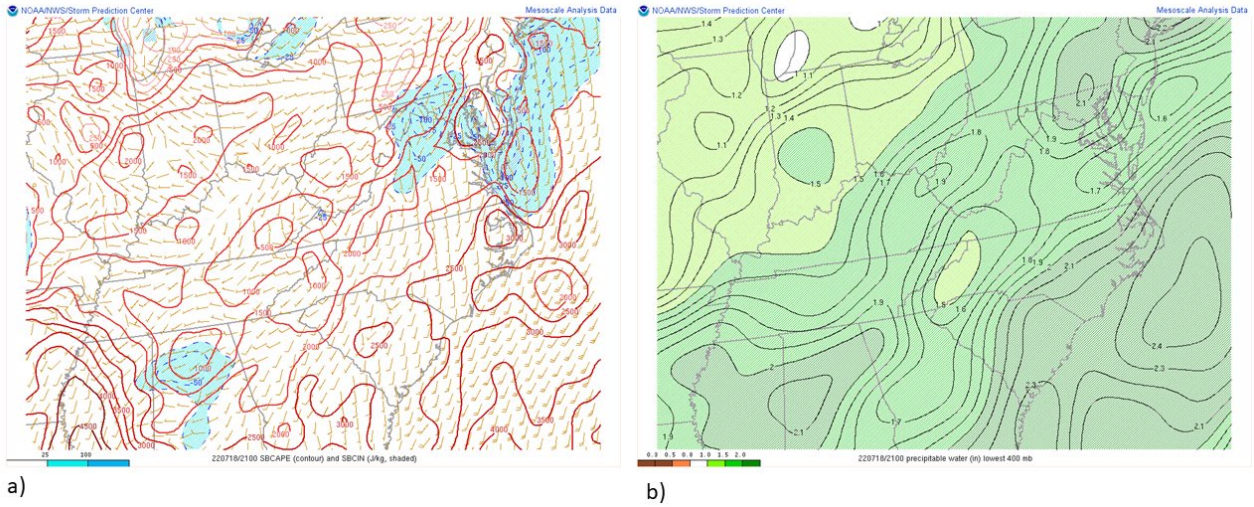

a) b)

Figure 32. SPC mesoanalysis of a) Surface-based Convective Potential Energy (CAPE), Surface-based Convective Inhibition (CIN) J/kg, and Wind (kt.) valid 2100 UTC 18 July 2022. b) Precipitable Water (in.) valid 2100 UTC 18 July 2022.

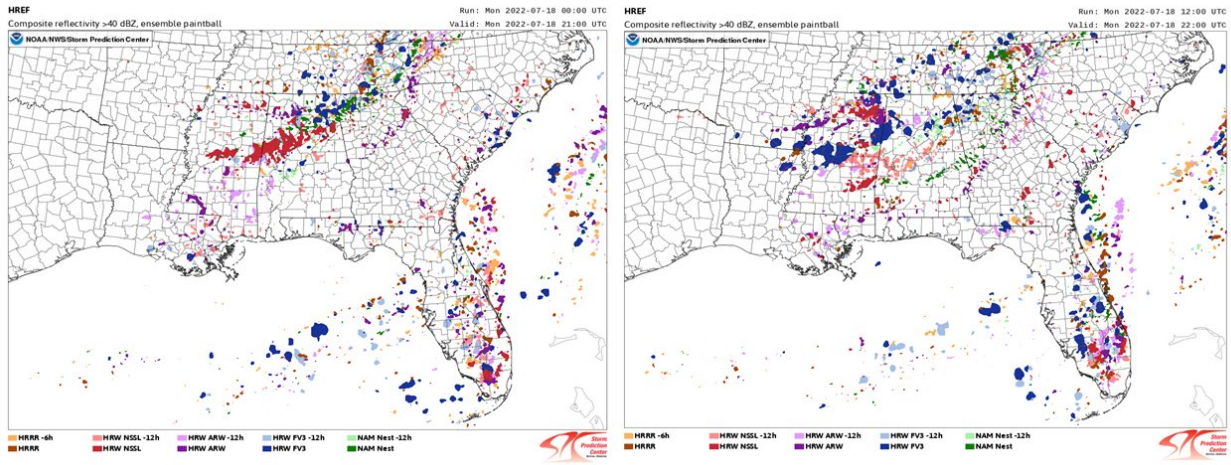

Figure 33. a) 0000 UTC 18 July 2022 run HREF Composite Reflectivity > 40 dBZ, ensemble paintball valid 2100 UTC 18 July 2022. b) 1200 UTC 18 July 2022 run HREF Composite Reflectivity > 40 dBZ, ensemble paintball valid 2100 UTC 18 July 2022.

.

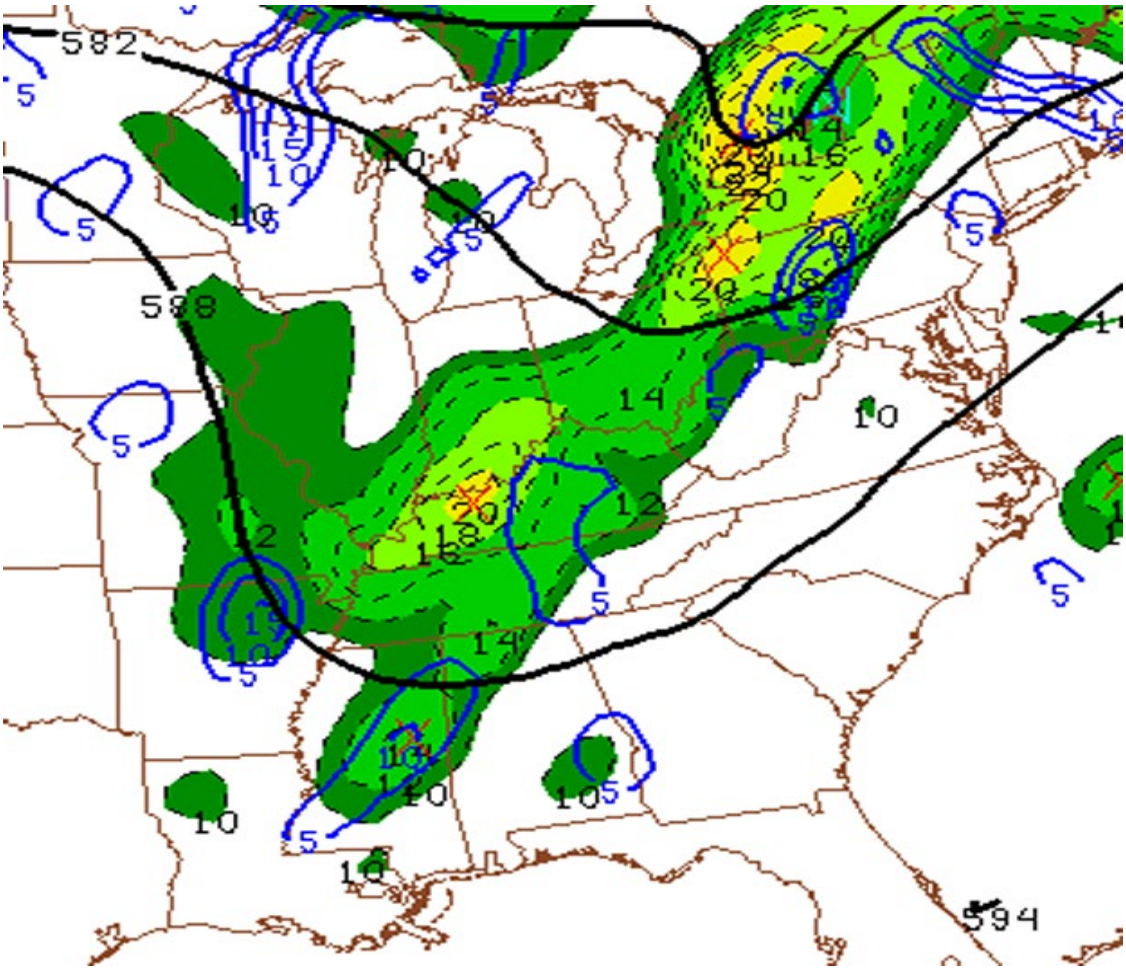

Figure 34. SPC mesoanalysis of 500mb Heights and Vorticity (fill), 700-400 mb Differential Vorticity Advection (blue) valid 2100 UTC 18 July 2022.

.

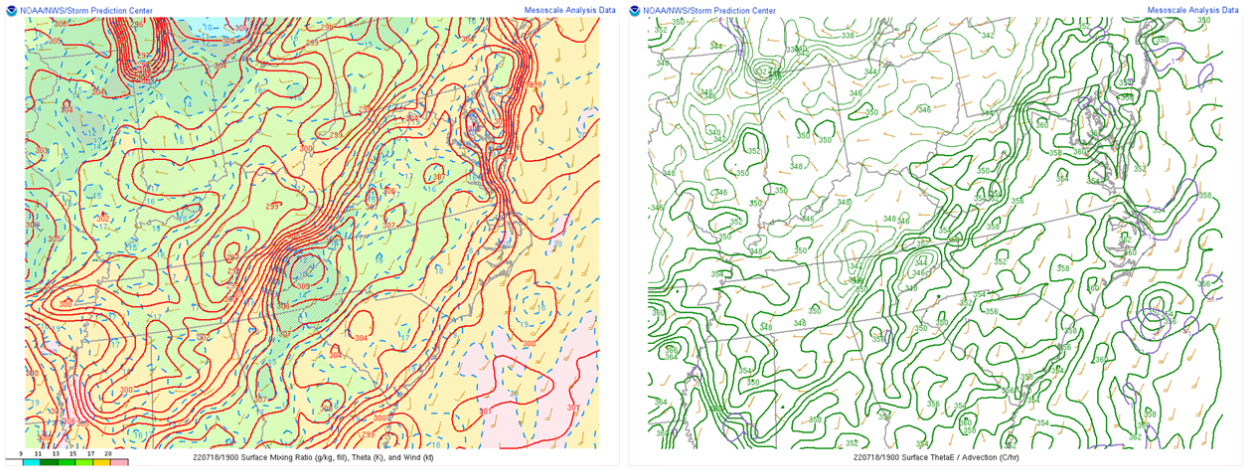

a) b)

Figure 35. SPC mesoanalysis of a) Surface Mixing Ratio (g/kg, fill), Theta (K), and Wind (kt.) valid 1900 UTC 18 July 2022. b) Surface Theta-e (K), Theta-e Advection (C/hr), and Wind (kt.) valid 1900 UTC 18 July 2022.

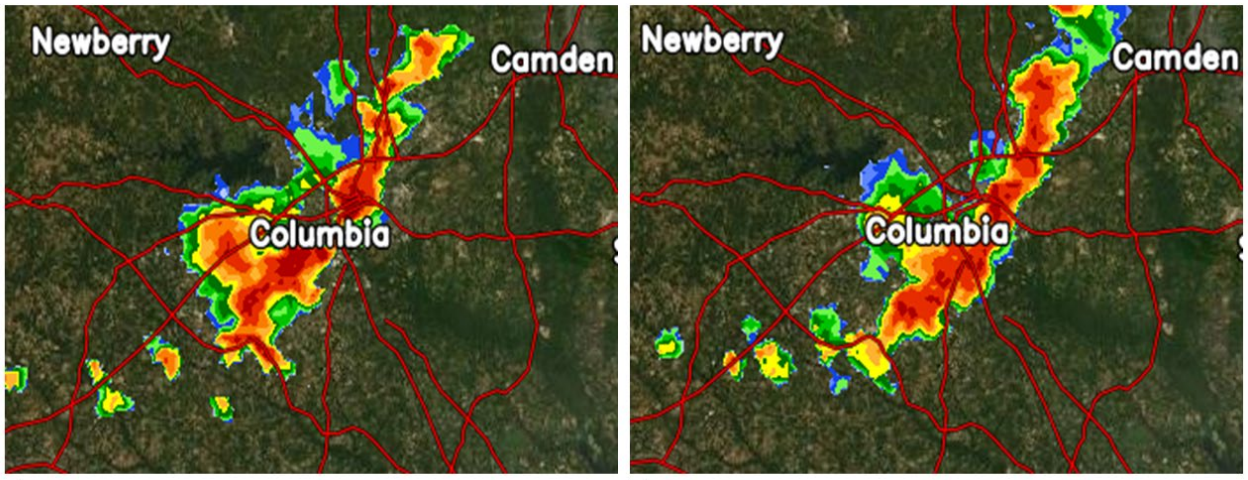

a) b)

Figure 36. a) MRMS Radar Reflectivity (lowest scan) valid 2050 UTC 18 July 2022.
b) MRMS Radar Reflectivity (lowest scan) valid 2110 UTC 18 July 2022.

TIME(UTC)	ROCA(in.)	MLK(in.)	RBWS1(ft.)	RBPS1(ft.)
2040	0.00	0.00	5.07	5.00
2045	0.02	0.00	4.99	4.88
2050	0.34	0.15	5.73	5.32
2055	**0.72**	**0.43**	**7.59**	**6.59**
2100	0.46	0.42	8.95	7.63
2105	0.25	0.45	**9.96**	8.60
2110	0.01	0.05	9.93	**8.64**
2115	0.00	0.00	9.82	8.57

Table 2. 18 July 2022 Rocky Branch flash flood case Woolpert 5 min. rainfall data at ROCA and MLK along with model stage height forecasts for RBWS1 and RBPS1. Decision time to issue a warning in red. Crest height forecast in purple. Actual Flash Flood Warning issued time in yellow.

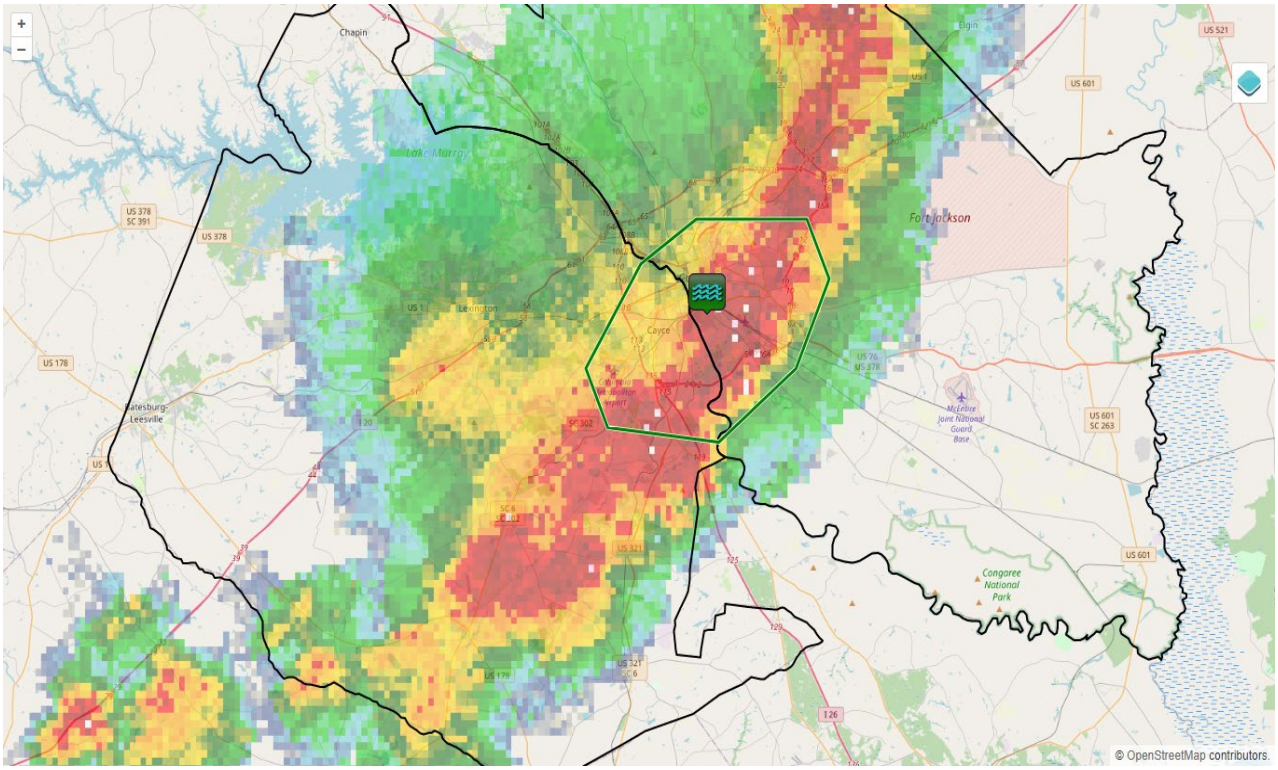

Figure 37. Radar Composite at Flash Flood Warning Issuance Time valid 2105 UTC 18 July 2022 with flash flooding reports.

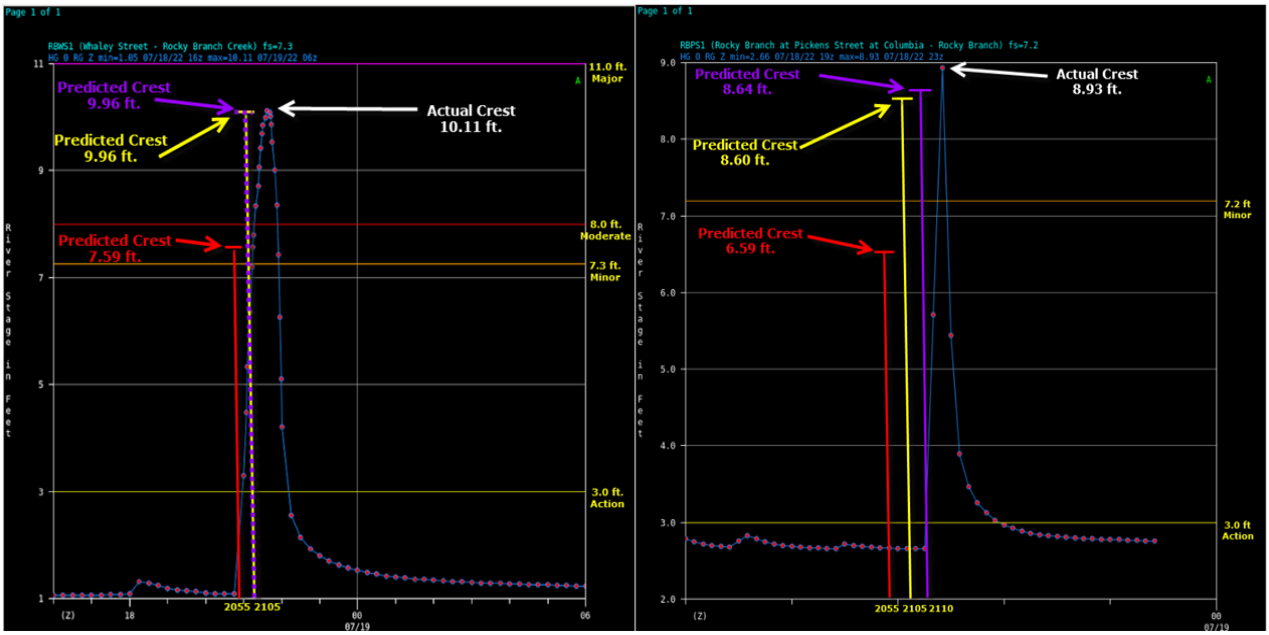

a) b)

Figure 38. a) 18 July 2022 Observed hydrograph at Whaley Street (RBWS1) with model crest forecast and times. Reasonable earliest time a flash flood warning could have been issued based on model output is denoted by the red-colored line. The flash flood warning issued time is denoted by the yellow-colored line, the time of maximum predicted crest is denoted by the purple-colored line, and the actual crest is denoted by the white arrow. b) 18 July 2022 Observed hydrograph at Pickens Street (RBPS1) with model crest forecast and times. Reasonable earliest time a flash flood warning could have been issued based on model output is denoted by the red-colored line. The flash flood warning issued time is denoted by the yellow-colored line, the time of maximum predicted crest is denoted by the purple-colored line, and the actual crest is denoted by the white arrow.

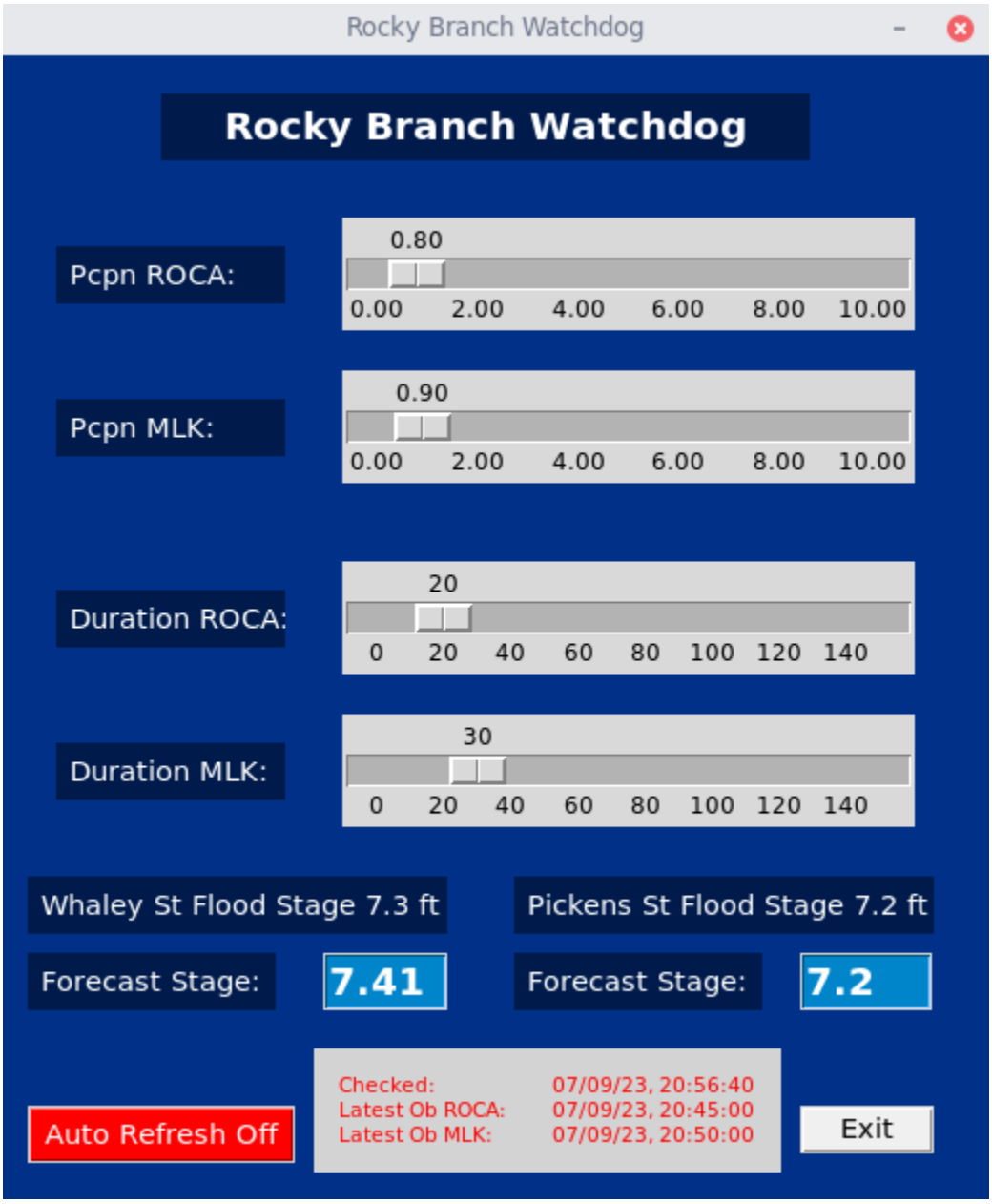

Figure 39. Rocky Branch Watchdog Python application. The tool automatically ingests predictor data and displays the forecast crest stages every 5 minutes.

Appendix 1. Table of all cases (events) that were included in the study. Note: cases depicted in red not included in the developmental data set.

Date	USGS RBWS1 Gage Height	Time of Crest (Z Time)	RBPS1 Gage Height	Woolpert Gage ROC-A	Time Heavy Rain Began (Z)	Duration (Minutes)	Woolpert Gage MLK	Time Heavy Rain Began (Z)	Duration (Minutes)	PW Value RAP Hr of Occurrence	Season (Meteorological Seasons 1-4)) Winter (1)-Fall (4)
3/30/2017	10.47	20:45		1.67	19:15	60	2	19:15	60	1.46	2
4/3/2017	6.42	21:30		0.59	20:05	70	0.56	20:10	60	1.64	2
4/5/2017	11.63	19:22		2.08	18:15	55	1.95	18:15	55	1.1	2
4/24/2017	10.29	4:45		1.7	3:40	60	1.56	3:45	60	1.62	2
5/5/2017	7.44	5:00		0.86	4:10	45	0.84	4:00	55	1.71	2
5/22/2017	5.22	22:30		0.46	21:15	65	0.52	21:50	35	2.01	2
5/22/2017	9.59	19:00		1.79	17:45	55	1.47	17:50	60	1.69	2
5/30/2017	5.28	0:30		0.7	23:45	30	0.32	23:45	35	1.87	2
6/15/2017	9.93	2:52		2	2:00	60	1.26	2:05	55	1.62	3
6/16/2017	8.78	4:15		1.23	3:25	55	1.25	3:25	55	1.71	3
7/10/2017	6.97	21:15		0.9	20:35	40	0.85	20:40	30	2.2	3
7/23/2017	12.15	23:30		2.52	20:40	90	3.52	20:40	60	2.2	3
7/24/2017	10.19	20:45		1.53	19:45	35	1.44	19:50	30	1.99	3
8/13/2017	5.52	20:45		0.55	20:00	25	0.45	20:00	25	2.3	3
8/13/2017	5.81	17:30		0.25	16:45	30	0.34	16:50	25	2.18	3
9/12/2017	5.86	0:30		0.77	23:30	55	0.6	23:30	55	2.17	4
9/12/2017	6.49	8:08		0.59	6:20	30	0.67	6:20	35	1.99	4
12/20/2017	5.68	19:53		0.41	19:15	25	0.38	19:15	25	1.57	1
3/20/2018	5.63	8:22		0.77	7:00	75	0.69	7:05	75	0.99	2
4/24/2018	6.71	8:45		0.89	7:45	60	0.83	7:50	55	0.96	2
5/15/2018	5.09	20:15		0.51	19:20	50	0.65	19:20	45	2.08	2
5/15/2018	7.73	18:23		1.01	17:50	20	1.16	17:50	20	2.05	2
6/12/2018	6.23	1:45		0.85	0:45	50	0.82	0:45	50	1.97	3

Date	USGS RBWS1 Gage Height	Time of Crest (Z Time)	RBPS1 Gage Height	Woolpert Gage ROC-A	Time Heavy Rain Began (Z)	Duration (Minutes)	Woolpert Gage MLK	Time Heavy Rain Began (Z)	Duration (Minutes)	PW Value RAP Hr of Occurrence	Season (Meteorological Seasons 1-4)) Winter (1)-Fall (4)
6/26/2018	6.28	1:15		0.79	0:30	40	0.66	0:35	40	1.91	3
6/27/2018	6.53	0:23		0.58	23:40	35	0.44	23:40	35	1.68	3
7/23/2018	5.85	18:15		1.35	17:25	125	1.21	17:20	120	1.89	3
7/25/2018	6.85	19:00		1.27	18:15	30	0.83	18:25	25	2.01	3
7/26/2018	5.84	1:00		1.04	0:05	50	0.73	0:20	35	1.97	3
9/18/2018	5.68	2:15	6.35	0.4	1:15	15	0.35	1:15	15	1.83	4
9/28/2018	5.29	2:15	5.9	0.3	1:35	35	0.35	1:35	35	1.95	4
10/11/2018	7.1	11:23	6.48	1.61	9:15	120	1.72	9:25	120	2.73	4
11/2/2018	5.44	20:00	6	0.37	19:15	20	0.38	19:15	20	1.67	4
11/13/2018	7.95	4:53	6.86	0.81	4:05	45	0.81	4:05	45	1.63	4
3/1/2019	6.07	20:15	6.26	0.62	19:10	55	0.61	19:15	50	1.37	2
3/4/2019	6.41	0:15	6.3	0.71	23:40	50	0.75	23:40	50	1.33	2
5/4/2019	5.08	21:08	5.5	0.67	20:05	60	0.74	20:05	60	1.91	2
6/6/2019	5.66	0:15	6.82	0.54	23:40	15	0.59	23:40	15	1.98	3
6/7/2019	6.64	19:45	6.98	0.51	18:05	30	0.42	18:05	30	2.04	3
6/7/2019	8.28	23:23	7.87	0.67	23:05	30	0.66	23:05	30	2.02	3
6/9/2019	6.87	22:45	6.93	0.74	22:00	50	1.33	22:00	75	2.22	3
6/22/2019	5.53	9:00	6.04	0.48	8:20	25	0.53	8:20	25	1.65	3
7/4/2019	6.33	21:00	6.63	0.8	20:20	45	0.78	20:20	45	2.08	3
7/13/2019	7.56	22:30	7.2	0.82	21:45	30	0.91	21:40	45	2.12	3
7/23/2019	7.08	20:00	6.9	1.09	19:20	75	1.05	19:25	70	2.19	3
8/22/2019	7.31	19:23	7.01	1.47	18:30	50	1.48	18:35	45	2.12	3
9/1/2019	5.76	22:45	6	0.81	22:10	50	0.93	22:05	55	1.31	4
10/1/2019	6.38	2:30	6.73	0.75	1:45	40	0.85	1:35	30	2.08	4

Date	USGS RBWS1 Gage Height	Time of Crest (Z Time)	RBPS1 Gage Height	Woolpert Gage ROC-A	Time Heavy Rain Began (Z)	Duration (Minutes)	Woolpert Gage MLK	Time Heavy Rain Began (Z)	Duration (Minutes)	PW Value RAP Hr of Ocurrance	Season (Meteorological Seasons 1-4)) Winter (1)-Fall (4)
1/3/2020	6.98	0:00	6.79	0.89	23:25	55	0.87	23:25	55	1.58	1
2/6/2020	6.64	21:37	6.42	0.52	21:00	30	0.51	21:00	30	1.86	1
4/13/2020	5.71	10:22	5.98	0.46	9:40	35	0.43	9:45	30	1.75	2
5/19/2020	5.28	4:30	5.91	1.1	3:40	120	1.29	3:40	130	1.8	2
5/19/2020	5.51	22:45	6.01	0.46	21:55	25	0.48	22:00	30	1.39	2
5/23/2020	8	5:45	7.51	0.8	5:05	20	0.89	5:05	20	1.88	2
5/29/2020	5.52	15:45	5.88	0.43	14:55	45	0.56	14:35	65	1.89	2
5/30/2020	9.39	1:15	8.5	1.44	0:35	30	1.37	0:40	25	1.89	2
5/30/2020	9.92	3:15	8.71	0.95	2:35	30	1.01	2:35	35	1.96	2
6/10/2020	6.99	2:00	6.78	0.86	1:25	35	0.72	1:20	35	1.83	3
6/11/2020	8.37	5:45	7.84	1.05	5:00	35	1.09	5:00	35	2.4	3
6/23/2020	5.94	22:00	6.51	0.69	21:15	40	0.66	21:15	40	2.19	3
6/24/2020	10.24	20:52	9.1	1.37	19:50	35	1.74	19:50	35	2.07	3
6/25/2020	5.96	11:45	5.86	0.79	10:15	85	0.79	10:15	85	2.12	3
7/29/2020	5.19	0:30	5.06	0.61	23:45	25	0.45	23:45	25	2.35	3
7/30/2020	6.11	0:37	5.48	0.91	23:05	70	0.53	23:05	65	2.51	3
8/20/2020	5.96	1:45	5.61	0.97	1:15	40	0.58	1:00	55	1.77	3
8/24/2020	5.68	21:00	5.57	0.79	19:50	65	0.73	19:50	70	2.16	3
9/15/2020	6.82	1:15	6.57	0.82	0:10	65	0.89	0:05	65	1.95	4
9/17/2020	7.96	16:22	7.06	1	15:30	60	0.88	15:35	65	2.33	4
11/26/2020	8.82	14:37	7.67	1.3	13:40	70	1.3	13:35	55	1.31	4
1/1/2021	5.12	23:45	5.5	0.39	23:05	25	0.43	23:00	30	1.81	1
2/16/2021	6.68	2:37	6.27	0.47	1:40	50	0.94	0:55	95	1.49	2
6/20/2021	5.19	20:45	5.76	0.52	20:05	30	0.49	20:05	0.49	2.28	3
7/16/2021	11.01	20:37	9.64	1.96	19:25	75	2.23	19:30	70	2.04	3
7/28/2021	9.02	0:07	8.11	1.2	23:20	45	1.42	23:20	45	1.81	3

Date	USGS RBWS1 Gage Height	Time of Crest (Z Time)	RBPS1 Gage Height	Woolpert Gage ROC-A	Time Heavy Rain Began (Z)	Duration (Minutes)	Woolpert Gage MLK	Time Heavy Rain Began (Z)	Duration (Minutes)	PW Value RAP Hr of Ocurrance	Season (Meteorological Seasons 1-4)) Winter (1)-Fall (4)
8/18/2021	5.21	5:15	5.73	0.63	3:20	55	0.58	3:20	55	2.51	3
8/20/2021	6.38	0:15	6.39	1.04	22:25	90	0.71	22:25	90	1.86	3
8/22/2021	7.57	16:15	7.23	0.94	15:15	65	0.97	15:20	55	2.42	3
8/22/2021	7.61	18:00	7.12	0.63	16:55	50	0.85	16:55	50	2.4	3
9/8/2021	5.51	20:00	5.97	0.81	19:15	40	0.83	19:15	40	2.24	4
9/15/2021	5.49	22:15	6.05	0.18	21:35	30	0.42	21:35	30	2.04	2
4/5/2022	5.27	23:00	7.68	0.32	22:20	20	0.34	22:20	20	1.77	2
4/5/2022	7.4	20:45	7.26	0.63	20:00	20	0.77	20:05	25	1.65	2
4/5/2022	8.05	19:00	5.89	1.14	17:55	45	1.21	17:55	50	1.56	2
5/21/2022	11.75	18:45	10.55	2.86	17:45	50	3.2	13:45	50	1.85	2
6/11/2022	7.38	18:45	6.9	1.05	18:00	40	1.05	18:00	40	1.6	3
6/16/2022	11.32	23:00	10.35	2.49	22:05	55	2.3	22:05	55	2.09	3
7/4/2022	12.9	22:37	13.43	4.5	21:30	65	4.58	21:25	60	2.33	3
7/9/2022	5.48	3:25	6.39	0.55	2:25	55	0.65	2:25	50	2.29	3
7/18/2022	10.11	21:37	8.93	1.42	16:45	25	1.5	16:45	25	2.05	3
8/12/2022	5.44	16:54	5.95	0.43	15:00	40	0.53	15:00	40	2.21	3
9/11/2022	5.79	2:44	6.11	0.59	1:55	50	0.66	1:55	45	2.18	4